

# Palmyrolide A, an Unusually Stabilized Neuroactive Macrolide from Palmyra Atoll Cyanobacteria

Alban R. Pereira, Zhengyu Cao, Niclas Engene, Irma E. Soria-Mercado, Thomas  
F. Murray, and William H. Gerwick\*  
[wgerwick@ucsd.edu](mailto:wgerwick@ucsd.edu)

Center for Marine Biotechnology and Biomedicine, Scripps Institution of Oceanography and Skaggs School  
of Pharmacy and Pharmaceutical Sciences, University of California San Diego, La Jolla, California 92037,  
Department of Pharmacology, Creighton University School of Medicine, Omaha, Nebraska 68178, and  
Facultad de Ciencias Marinas, Universidad Autonoma de Baja California, Ensenada, BC, 22830, Mexico

## Contents

Page S3: General Experimental Procedures
Page S3: Biological Material
Page S5: Maximum-likelihood (PhyML) phylogenetic analysis of the <i>Leptolyngbya/Oscillatoria</i> consortium PAL08-3 based on SSU (16S) rRNA nucleotide sequences.
Page S6: Morphological Characterization
Page S6: DNA Extraction, PCR and Cloning
Page S6: Phylogenetic Inference
Page S7: Extraction and Isolation of <b>1</b>
Page S7: Ozonolysis, Acid Hydrolysis and Chiral Analysis of <b>1</b>
Page S8: Example for the Isolation of <b>2</b>
Page S9: NMR spectroscopic data (500 MHz, CDCl <sub>3</sub> ) of byproduct <b>2</b>
Page S10: Mechanistic proposal for the formation of <b>2</b> in acidic media
Page S11: <sup>1</sup> H NMR spectrum of Palmyrolide A ( <b>1</b> ) (in CDCl <sub>3</sub> at 600 MHz)
Page S12: Partial <sup>1</sup> H NMR spectrum of Palmyrolide A ( <b>1</b> ) (in CDCl <sub>3</sub> at 600 MHz)
Page S13: Partial <sup>1</sup> H NMR spectrum of Palmyrolide A ( <b>1</b> ) (in CDCl <sub>3</sub> at 600 MHz)
Page S14: <sup>13</sup> C NMR spectrum of Palmyrolide A ( <b>1</b> ) (in CDCl <sub>3</sub> at 125 MHz)
Page S15: DQF-COSY spectrum of Palmyrolide A ( <b>1</b> ) (in CDCl <sub>3</sub> at 600 MHz)
Page S16: HSQC spectrum of Palmyrolide A ( <b>1</b> ) (in CDCl <sub>3</sub> at 600 MHz)
Page S17: HMBC spectrum of Palmyrolide A ( <b>1</b> ) (in CDCl <sub>3</sub> at 600 MHz)
Page S18: NOESY spectrum of Palmyrolide A ( <b>1</b> ) (in CDCl <sub>3</sub> at 600 MHz)
Page S19: <sup>1</sup> H NMR spectrum of <b>2</b> (in CDCl <sub>3</sub> at 600 MHz)
Page S20: DQF-COSY spectrum of <b>2</b> (in CDCl <sub>3</sub> at 600 MHz)
Page S21: HSQC spectrum of <b>2</b> (in CDCl <sub>3</sub> at 600 MHz)
Page S22: HMBC spectrum of <b>2</b> (in CDCl <sub>3</sub> at 600 MHz)
Page S23: <sup>1</sup> H NMR spectrum of the Palmyrolide A derivative <b>4</b> (in CDCl <sub>3</sub> at 500 MHz)
Page S24: <sup>13</sup> C NMR spectrum of the Palmyrolide A derivative <b>4</b> (in CDCl <sub>3</sub> at 125 MHz)
Page S25: <sup>1</sup> H NMR spectrum of standard (2 <i>R</i> ,1' <i>S</i> ,1'' <i>S</i> )- <b>4</b> (in CDCl <sub>3</sub> at 500 MHz)
Page S26: <sup>13</sup> C NMR spectrum of standard (2 <i>R</i> ,1' <i>S</i> ,1'' <i>S</i> )- <b>4</b> (in CDCl <sub>3</sub> at 125 MHz)

- Page S27:  $^1\text{H}$  NMR spectrum of standard (2*S*,1'*S*,1''*S*)-**4** (in  $\text{CDCl}_3$  at 500 MHz)
- Page S28:  $^{13}\text{C}$  NMR spectrum of standard (2*S*,1'*S*,1''*S*)-**4** (in  $\text{CDCl}_3$  at 125 MHz)
- Page S29: Comparison of  $^1\text{H}$  NMR spectra for derivative **4**, standard (2*R*,1'*S*,1''*S*)-**4**, and standard (2*S*,1'*S*,1''*S*)-**4** (in  $\text{CDCl}_3$  at 500 MHz).
- Page S30: Comparison of key  $^1\text{H}$  NMR resonances for derivative **4**, standard (2*R*,1'*S*,1''*S*)-**4**, and standard (2*S*,1'*S*,1''*S*)-**4** (in  $\text{CDCl}_3$  at 500 MHz).
- Page S31: Concentration-response profile for palmyrolide A (**1**)-induced suppression in the frequency of spontaneous  $\text{Ca}^{2+}$  oscillations in mouse cerebrocortical neurons.
- Page S31: Concentration-response profile for palmyrolide A (**1**)- and tetrodotoxin-induced suppression of sodium overload in mouse neuroblastoma (neuro2a) cells.
- Page S32: References

## General Experimental Procedures

UV and IR spectra were recorded on a Beckman DU 800 UV spectrophotometer and a Nicolet 100 FT-IR spectrophotometer, respectively.  $^1\text{H}$ ,  $^{13}\text{C}$  and 2D NMR spectra were collected either at a  $^1\text{H}$  resonance frequency of 600 MHz (Bruker Avance III DRX600), or 500 MHz (Jeol ECA500, Varian INOVA 500 and Varian VX500). The Bruker DRX600 was equipped with a 1.7 mm TCI cryoprobe, whereas the Varian VX500 with a 3 mm Varian XSens cold probe. Chemical shifts were calibrated internally to the residual signal of the solvent in which the sample was dissolved ( $\text{CDCl}_3$ :  $\delta$  7.24  $^1\text{H}$ -NMR;  $\delta$  77.0  $^{13}\text{C}$  NMR). High resolution mass spectra were obtained on a ThermoFinnigan MAT900XL mass spectrometer. LC-MS data was acquired on a ThermoFinnigan Surveyor Plus PDA and pump array, equipped with a LCQ Advantage Max mass detector. Vacuum and flash chromatographic separations were performed using type H (10-40  $\mu$ , Aldrich) silica and silica gel 60 (40-63  $\mu$ , EMD), respectively. Merck EMD aluminum- and glass-supported TLC sheets (silica gel 60  $\text{F}_{254}$ ) were used for analytical and preparative TLC, respectively. The (*R*)-(-)-2-methylglutaric and (*S*)-(-)-2-methylglutaric acids were acquired from TCI America. All solvents were purchased as HPLC grade.

## Biological Material

The specimen PAL08-3 (voucher specimen available from WHG as collection number PAL8-15-08-3) was collected as a red gelatinous puff ball shaped algae (Fig. S1A), at a depth of 1–2 m from the northwest end of Paradise Island, Palmyra Atoll, on August 2008 (05° 52.706 N, 162° 05.955 W). A selection of filaments were preserved in RNA stabilization reagent (RNAlater® from Ambion Inc.), whereas the bulk of the collection was stored in 50% EtOH/sea water at -20°C prior to extraction. Microscopic characterization revealed that the specimen was composed of a consortium of two distinctly different filamentous cyanobacteria (Fig. S1B). The bulk of the algae biomass was composed of an entangled fine filamentous cyanobacterium (PAL08-3.1; Fig. S1C). PAL08-3.1 corresponded with the *Leptolyngbya* morpho-type with thin entangled filaments (2-3  $\mu\text{m}$  wide) and barrel-shaped cells enclosed in thin sheaths. Embedded within the fine filaments of the *Leptolyngbya cf. sp.* PAL08-3.1 were larger reddish filaments corresponding to the *Lyngbya/Oscillatoria* morpho-type (PAL08-3.2; Fig. S1D). The PAL08-3.2 filaments were 22-25  $\mu\text{m}$  wide with disk-shaped cells with small cell wall constrictions and thin barely visible sheaths.

A phylogenetic analysis based on the SSU (16S) rRNA genes revealed that the two specimens PAL08-3.1 and PAL08-3.2 were evolutionary distant. The PAL08-3.1 was closest related to other strains of *Leptolyngbya* confirming the morphology based identification. Although cladding with other *Leptolyngbya*, this strain has more than 9% sequence divergence with other members of this group

including the type-strain PCC 7375<sup>T</sup>. The current genus *Leptolyngbya* is a highly polyphyletic group and this clearly evolutionary distinct strain PAL08-3.1 may represent a unique group in need of further description. The strain PAL08-3.2 claded within the *Trichodesmium-Oscillatoria* lineage. This phylogenetic positioning in relation to the *Oscillatoria* type-strain PCC 75115 clarified its identity as a species of *Oscillatoria* rather than belonging to the morphological similar genus *Lyngbya*. Since the related laingolide analogues<sup>1</sup> initially were described from a *Lyngbya* that was described solely by morphology rather than with the inclusion of phylogenetic analysis, it may be speculated that these molecules were in fact isolated from an *Oscillatoria* sp.

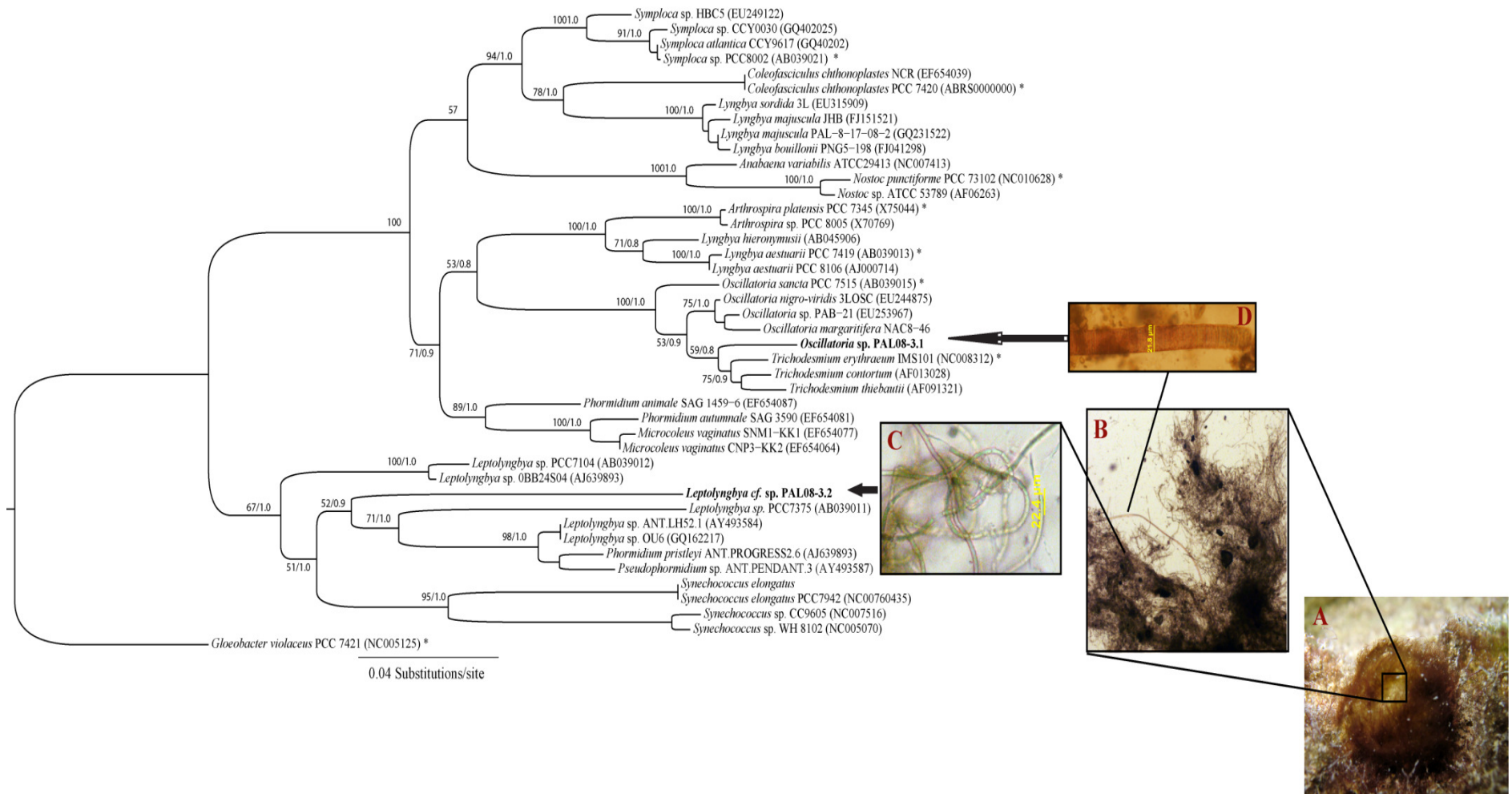


**Figure S1.** Maximum-likelihood (PhyML) phylogenetic analysis of the *Leptolyngbya/Oscillatoria* consortium PAL08-3 based on SSU (16S) rRNA nucleotide sequences. The specimens are indicated as species, strain, and acc. nr in brackets. Specimens designated with an asterisk represent type-strains obtained from *Bergey's Manual*.<sup>2</sup> The support values are indicated as boot-strap (PhyML) and posterior probability (MrBayes). The scale bar is indicated at 0.04 nucleotide substitutions per site. (A) Red gelatinous puff ball shaped algae. (B) Consortium of two different filamentous cyanobacteria. (C) Fine filamentous cyanobacterium that corresponded with the *Leptolyngbya* morpho-type. (D) Larger and reddish filaments corresponding to the *Lyngbya/Oscillatoria* morpho-type.

## Morphological Characterization

Morphological characterizations were performed using an Olympus IX51 epifluorescent microscope (100X) equipped with an Olympus U-CMAD3 camera. Measurements were provided as: mean  $\pm$  standard deviation (SD). The filament means were the average of three filament measurements and cell measurements the average of ten adjacent cells of three filaments. Taxonomic identification of cyanobacterial specimens was performed in accordance with modern taxonomic systems.<sup>3</sup>

## DNA Extraction, PCR and Cloning

Cyanobacterial specimens (~200 mg) was preserved for genetic analysis in 10 mL RNAlater® (Ambion Inc., Austin, TX, USA) at -20 °C. Cyanobacterial filaments were cleaned and pretreated using TE (10 mM Tris; 0.1M EDTA; 0.5% SDS; 20  $\mu\text{g}\cdot\text{mL}^{-1}$  RNase)/lysozyme (1  $\text{mg}\cdot\text{mL}^{-1}$ ) at 37 °C for 30 min followed by incubation with proteinase K (0.5  $\text{mg}\cdot\text{mL}^{-1}$ ) at 50 °C for 1 h. Genomic DNA was extracted from ~40 mg of cyanobacterial filaments using the Wizard® Genomic DNA Purification Kit (Promega) following the manufacturer's specifications. The isolated DNA was further purified using a Genomic-tip 20/G kit (Qiagen). DNA concentration and purity was measured on a DU® 800 spectrophotometer (Beckman Coulter) at a 1:10 dilution. The 16S rRNA genes were PCR-amplified using the lineage-specific primers (106F 5'-CGGACGGGTGAGTAACGCGTGA-3'; 1445R 5'-GGTAACGACTTCGGGCGTG-3'). The PCR reaction volumes were 25  $\mu\text{L}$  containing 0.5  $\mu\text{L}$  (~50 ng) of DNA, 2.5  $\mu\text{L}$  of 10 x PfuUltra IV reaction buffer, 0.5  $\mu\text{L}$  (25 mM) of dNTP mix, 0.5  $\mu\text{L}$  of each primer (10  $\mu\text{M}$ ), 0.5  $\mu\text{L}$  of PfuUltra IV fusion HS DNA polymerase and 20.5  $\mu\text{L}$  dH<sub>2</sub>O. The PCR reactions were performed in an Eppendorf® Mastercycler® gradient as follows: initial denaturation for 2 min at 95°C, 25 cycles of amplification: 20 sec at 95°C, 20 sec at 50°C and 1.5 min at 72°C, and final elongation for 3 min at 72°C. PCR-products were analyzed on a (1%) agarose-gel in SB-buffer and visualized by EtBr-staining. PCR products were subcloned using the Zero Blunt® TOPO® PCR Cloning Kit (Invitrogen) into the pCR®-Blunt IV TOPO® vector, and then transformed into TOPO® cells and cultured on LB-kanamycin plates. Plasmid DNA was isolated using the QIAprep® Spin Miniprep Kit (Qiagen) and sequenced with M13F/M13R primers. The gene sequences are available in the DDBJ/EMBL/GenBank databases under the following acc. No.: HM585025 (PAL08-3.2) and HM585026 (PAL08-3.1).

## Phylogenetic Inference

All gene sequences were aligned using MUSCLE v4.0<sup>4</sup> and refined using the SSU secondary structures model for *Escherichia coli* J01695.<sup>5</sup> The evolutionary histories of the cyanobacterial genes were inferred using Maximum likelihood (ML) and Bayesian inference algorithms. Appropriate nucleotide

substitution models were selected using corrected/uncorrected Akaike information criterion (AIC) and Bayesian information criterion (BIC) in Modeltest 3.7.<sup>6</sup> The Maximum likelihood (ML) inference was performed using PhyML v2.4.4.<sup>7</sup> The analysis was run using the GTR+I+G model (selected by AIC and BIC criteria) assuming a heterogeneous substitution rates and gamma substitution of variable sites (proportion of invariable sites (pINV) = 0.419, shape parameter ( $\alpha$ ) = 0.414, number of rate categories = 4). Bootstrap resampling was performed on 500 replicates. Bayesian analysis was conducted using MrBayes 3.1.<sup>8</sup> The Bayesian inference was performed using the GTR+I+G substitution model (pINV = 0.450,  $\alpha$  = 0.449, number of rate categories = 4) with Markov chains (one cold and three heated) ran for 3,000,000 generations. The first 25% were discarded as burn-in and the following data set were being sampled with a frequency of every 100 generations.

### Extraction and Isolation of **1**

Approximately 52.1 g (dry wt) of the cyanobacteria were extracted repeatedly with CH<sub>2</sub>Cl<sub>2</sub>/MeOH (2:1) to afford 0.3867 g of crude extract. A portion of this material (0.2768 g) was fractionated by silica gel vacuum liquid chromatography using a stepwise gradient solvent system of increasing polarity (EtOAc in hexanes mixtures) starting from 100% hexanes to 100% MeOH, to produce nine fractions (A-I). The bioactive fraction D (0.1344 g) was subjected to a <sup>1</sup>H NMR and bioassay-guided fractionation comprised of two silica gel columns (both gradient 0-100% EtOAc in hexanes), and preparative TLC (0.2:1 EtOAc/hexanes), to yield 10.2 mg of compound **1**. Palmyrolide A (**1**): colorless oil; [ $\alpha$ ]<sub>D</sub><sup>23</sup> -29 (c 0.9, CHCl<sub>3</sub>); UV (MeCN)  $\lambda_{\text{max}}$  232 nm (log  $\epsilon$  3.95); IR (neat) 2961, 1724, 1674, 1465, 1383, 1126, 938 cm<sup>-1</sup>; <sup>1</sup>H and <sup>13</sup>C NMR data, see Table 1; HRESIMS *m/z* [M+H]<sup>+</sup> 338.2687 (calcd for C<sub>20</sub>H<sub>36</sub>NO<sub>3</sub>, 338.2690).

### Ozonolysis, Acid Hydrolysis and Chiral Analysis of **1**

Ozone was bubbled through a sample of **1** (5.0 mg) dissolved in CH<sub>2</sub>Cl<sub>2</sub> (3 mL) at 25 °C for 15 min. The solvent was evaporated and the residue treated with 2 mL of H<sub>2</sub>O<sub>2</sub>-HCOOH (1:2) at 70 °C for 20 min. After removal of solvent *in vacuo*, the ozone treated and oxidized sample of **1** was hydrolyzed in degassed 6 M HCl (2 mL) at 110 °C for 5 h. The hydrolysate was concentrated to dryness, reconstituted in (*S*)-(+)-2-octanol (300  $\mu$ L), treated with acetyl chloride (150 $\mu$ L), and stirred at 110 °C for 4 h. After all volatiles were removed using a stream of N<sub>2</sub>, silica gel column chromatography (40% EtOAc/hexanes) of the remaining residue afforded pure derivative **4** (2.7 mg) as a colorless oil. **4**: [ $\alpha$ ]<sub>D</sub><sup>23</sup> -28 (c 0.13, CH<sub>3</sub>CN); <sup>1</sup>H NMR (CDCl<sub>3</sub>, 500 MHz)  $\delta$  4.89 (2H, qdd, *J* = 6.5, 6.0, 6.0 Hz), 2.44 (1H, qdd, *J* = 7.5, 7.0, 7.0 Hz), 2.30 (2H, m), 1.95 (1H, m), 1.75 (1H, m), 1.56 (2H, m), 1.46 (2H, m), 1.34-1.23 (16H, m), 1.20 (3H, d, *J* = 6.5 Hz), 1.19 (3H, d, *J* = 6.0 Hz), 1.16 (3H, d, *J* = 7.0 Hz), 0.88 (6H, t, *J* = 7.5 Hz); <sup>13</sup>C NMR (CDCl<sub>3</sub>, 125

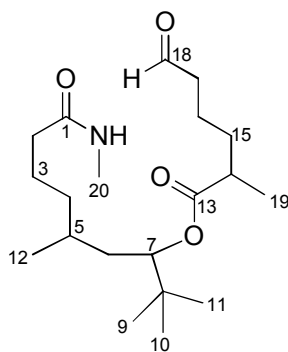
MHz)  $\delta$  175.7 (C), 172.8 (C), 71.0 (CH), 70.9 (CH), 39.0 (CH), 35.92 (CH<sub>2</sub>), 35.90 (CH<sub>2</sub>), 32.3 (CH<sub>2</sub>), 31.7 (2CH<sub>2</sub>), 29.11 (CH<sub>2</sub>), 29.10 (CH<sub>2</sub>), 28.7 (CH<sub>2</sub>), 25.35 (CH<sub>2</sub>), 25.34 (CH<sub>2</sub>), 22.6 (2CH<sub>3</sub>), 20.0 (CH<sub>2</sub>), 19.9 (CH<sub>2</sub>), 17.1 (CH<sub>3</sub>), 14.0 (2CH<sub>3</sub>); HRESIMS  $m/z$  [M+Na]<sup>+</sup> 393.2981 (calcd for C<sub>22</sub>H<sub>42</sub>O<sub>4</sub>Na, 393.2975).

The same derivatization and purification procedures were used with enantiomerically pure samples of (*R*)-(-)-2-methylglutaric (5.0 mg) and (*S*)-(-)-2-methylglutaric (5.1 mg) acid, to produce standards (2*R*,1'*S*,1''*S*)-**4** (2.0 mg) and (2*S*,1'*S*,1''*S*)-**4** (2.4 mg) also as a colorless oils. Comparison of NMR and specific rotation data led to assign an *R*-configuration at C14 in **1**. (2*R*,1'*S*,1''*S*)-**4**: [ $\alpha$ ]<sub>D</sub><sup>23</sup> -18 (c 0.10, CH<sub>3</sub>CN); <sup>1</sup>H NMR (CDCl<sub>3</sub>, 500 MHz)  $\delta$  4.89 (2H, qdd, *J* = 6.5, 6.5, 6.0 Hz), 2.44 (1H, qdd, *J* = 7.0, 7.0, 7.0 Hz), 2.30 (2H, m), 1.95 (1H, m), 1.75 (1H, m), 1.56 (2H, m), 1.46 (2H, m), 1.34-1.23 (16H, m), 1.20 (3H, d, *J* = 6.0 Hz), 1.19 (3H, d, *J* = 6.0 Hz), 1.16 (3H, d, *J* = 7.0 Hz), 0.88 (6H, t, *J* = 7.0 Hz); <sup>13</sup>C NMR (CDCl<sub>3</sub>, 125 MHz)  $\delta$  175.7 (C), 172.8 (C), 71.0 (CH), 70.9 (CH), 39.0 (CH), 35.91 (CH<sub>2</sub>), 35.89 (CH<sub>2</sub>), 32.3 (CH<sub>2</sub>), 31.7 (2CH<sub>2</sub>), 29.1 (CH<sub>2</sub>), 29.08 (CH<sub>2</sub>), 28.7 (CH<sub>2</sub>), 25.35 (CH<sub>2</sub>), 25.34 (CH<sub>2</sub>), 22.6 (2CH<sub>3</sub>), 20.0 (CH<sub>2</sub>), 19.9 (CH<sub>2</sub>), 17.1 (CH<sub>3</sub>), 14.0 (2CH<sub>3</sub>); HRESIMS  $m/z$  [M+Na]<sup>+</sup> 393.2979 (calcd for C<sub>22</sub>H<sub>42</sub>O<sub>4</sub>Na, 393.2975). (2*S*,1'*S*,1''*S*)-**4**: [ $\alpha$ ]<sub>D</sub><sup>23</sup> +30 (c 0.17, CH<sub>3</sub>CN); <sup>1</sup>H NMR (CDCl<sub>3</sub>, 500 MHz)  $\delta$  4.90 (2H, qdd, *J* = 6.5, 6.5, 6.0 Hz), 2.43 (1H, qdd, *J* = 7.0, 7.0, 7.0 Hz), 2.30 (2H, m), 1.95 (1H, m), 1.75 (1H, m), 1.56 (2H, m), 1.45 (2H, m), 1.33-1.23 (16H, m), 1.19 (6H, d, *J* = 6.5 Hz), 1.16 (3H, d, *J* = 7.5 Hz), 0.88 (6H, t, *J* = 7.0 Hz); <sup>13</sup>C NMR (CDCl<sub>3</sub>, 125 MHz)  $\delta$  175.7 (C), 172.8 (C), 71.0 (CH), 70.9 (CH), 39.1 (CH), 35.91 (CH<sub>2</sub>), 35.88 (CH<sub>2</sub>), 32.3 (CH<sub>2</sub>), 31.7 (2CH<sub>2</sub>), 29.1 (CH<sub>2</sub>), 29.09 (CH<sub>2</sub>), 28.7 (CH<sub>2</sub>), 25.37 (CH<sub>2</sub>), 25.36 (CH<sub>2</sub>), 22.6 (2CH<sub>3</sub>), 20.0 (CH<sub>2</sub>), 19.9 (CH<sub>2</sub>), 17.1 (CH<sub>3</sub>), 14.1 (2CH<sub>3</sub>); HRESIMS  $m/z$  [M+Na]<sup>+</sup> 393.2980 (calcd for C<sub>22</sub>H<sub>42</sub>O<sub>4</sub>Na, 393.2975).

### Example for the Isolation of **2**

A sample of **1** (5.0 mg) in MeOH (2 mL) was treated with HCl 6M (5  $\mu$ L) and stirred overnight at 25°C. Silica gel column chromatography (90% EtOAc/hexanes to 10% MeOH/EtOAc) afforded pure **2** (0.5 mg, 10%) as the main reaction product. Compound **2**: colorless oil; <sup>1</sup>H and <sup>13</sup>C NMR data, see Table S1; HRESIMS  $m/z$  [M+Na]<sup>+</sup> 378.2618 (calcd for C<sub>20</sub>H<sub>37</sub>NO<sub>4</sub>Na, 378.2615).



Table S1. NMR spectroscopic data (500 MHz, CDCl<sub>3</sub>) of byproduct **2**.

Carbon	$\delta_c^a$	Type	$\delta_H$ mult ( <i>J</i> in Hz) <sup>b</sup>	HMBC <sup>c</sup>	COSY
1	173.4				
1NH			6.04 bs		20
2a	35.4	CH <sub>2</sub>	2.08 ddd (7.4, 8.0, 13.7)	1, 3, 4	2b, 3b
2b			2.18 ddd (6.3, 7.4, 14.0)	1, 3, 4	2a, 3a, 3b
3a	22.4	CH <sub>2</sub>	1.46 m	1, 4, 5	2b, 3b, 4a
3b			1.77 m	4	2a, 2b, 3a
4a	33.8	CH <sub>2</sub>	1.00 m	2, 3, 5	3a, 4b, 5
4b			1.46 m	2, 3, 5, 6	4a, 5
5	28.1	CH	1.25 m	3, 4, 6	4a, 4b, 12
6a	36.9	CH <sub>2</sub>	1.35 ddd (2.3, 9.8, 14.3)	4, 5, 7	5, 6b, 7
6b			1.40 ddd (3.4, 10.3, 14.3)	4, 5, 7	5, 6a, 7
7	78.1	CH	4.76 dd (2.2, 9.8)	5, 8, 9/10/11, 13	6a, 6b
8	33.8				
9/10/11	25.4	3xCH <sub>3</sub>	0.87 s	7, 8	
12	20.2	CH <sub>3</sub>	0.88 d (6.9)	4, 5, 6	5
13	176.1				
14	39.3	CH	2.47 m	13, 15, 19	15a, 15b, 19
15a	32.4	CH <sub>2</sub>	1.43 m	13, 16	14, 15b, 16
15b			1.71 m	14, 16, 19	14, 15a, 16
16	19.2	CH <sub>2</sub>	1.64 m	15, 17, 18	15a, 15b, 17
17	43.0	CH <sub>2</sub>	2.47 t (6.8)	15, 16, 18	16, 18
18	201.6		9.77 t (1.7)	16, 17	17
19	16.9	CH <sub>3</sub>	1.18 d (7.4)	13, 14, 15	14
20	25.8	CH <sub>3</sub>	2.82 d (4.6)	1	1NH

<sup>a</sup>Recorded at 125 MHz. <sup>b</sup>Recorded at 500 MHz. <sup>c</sup>From proton to the indicated carbon.

Figure S2. Mechanistic proposal for the formation of **2** in acidic media.

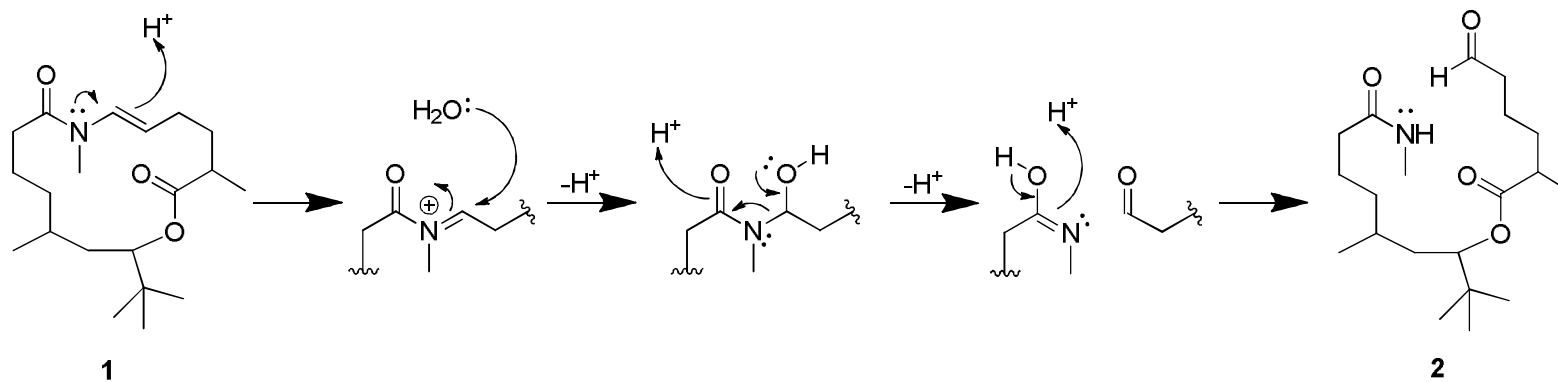


Figure S3.  $^1\text{H}$  NMR spectrum of Palmyrolide A (**1**) (in  $\text{CDCl}_3$  at 600 MHz).

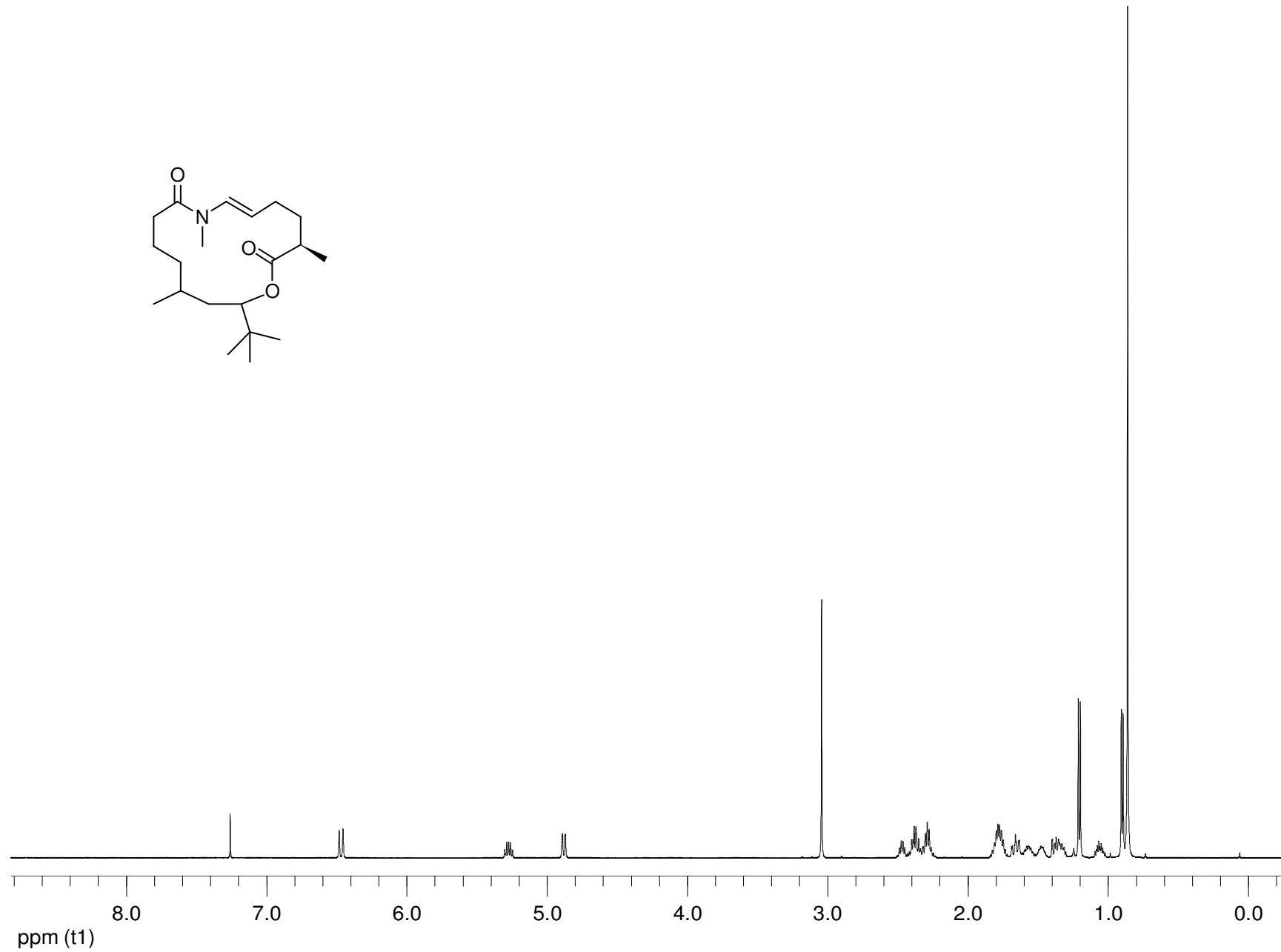


Figure S4. Partial  $^1\text{H}$  NMR spectrum of Palmyrolide A (**1**) (in  $\text{CDCl}_3$  at 600 MHz).

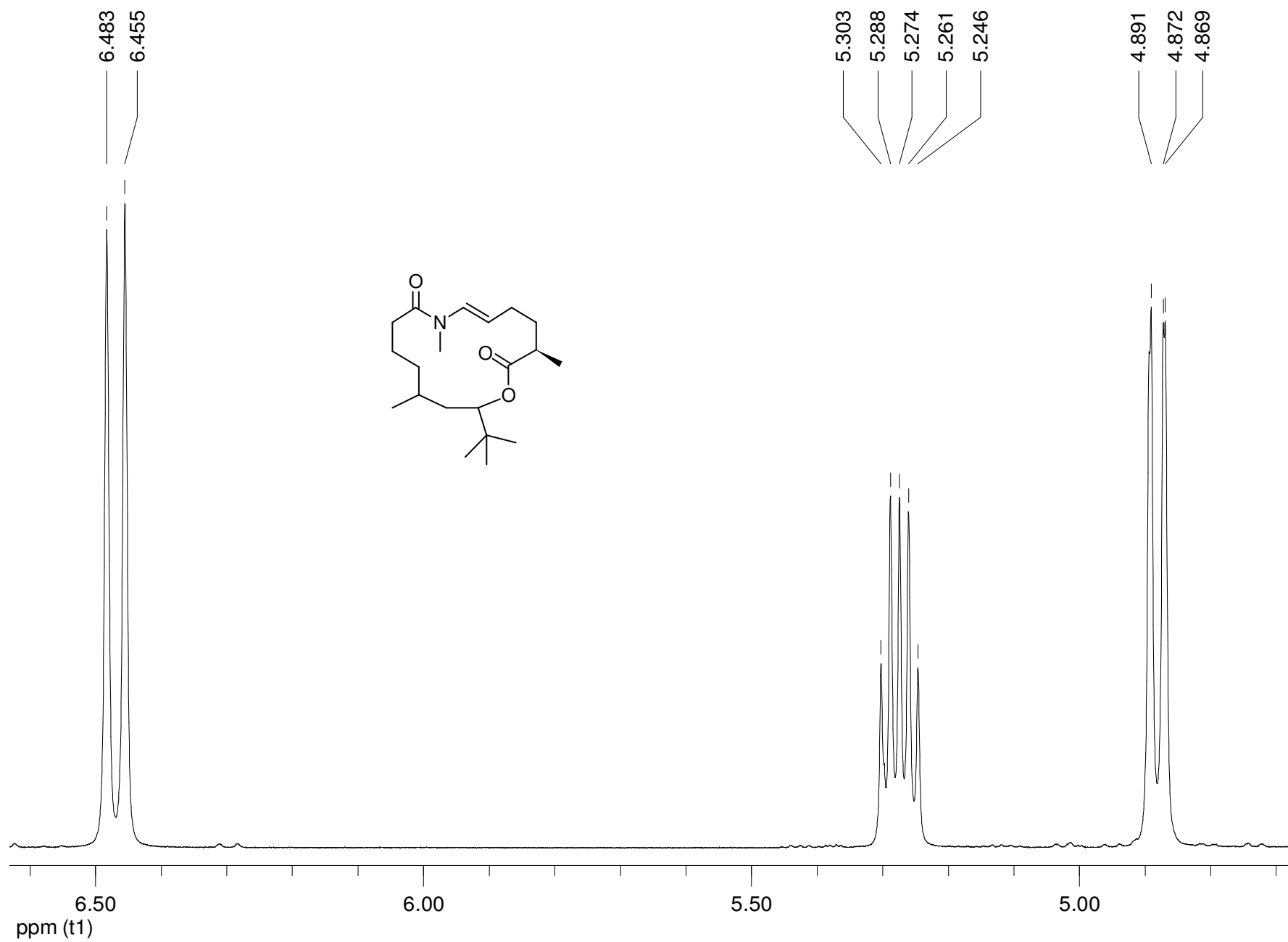


Figure S5. Partial  $^1\text{H}$  NMR spectrum of Palmyrolide A (**1**) (in  $\text{CDCl}_3$  at 600 MHz).

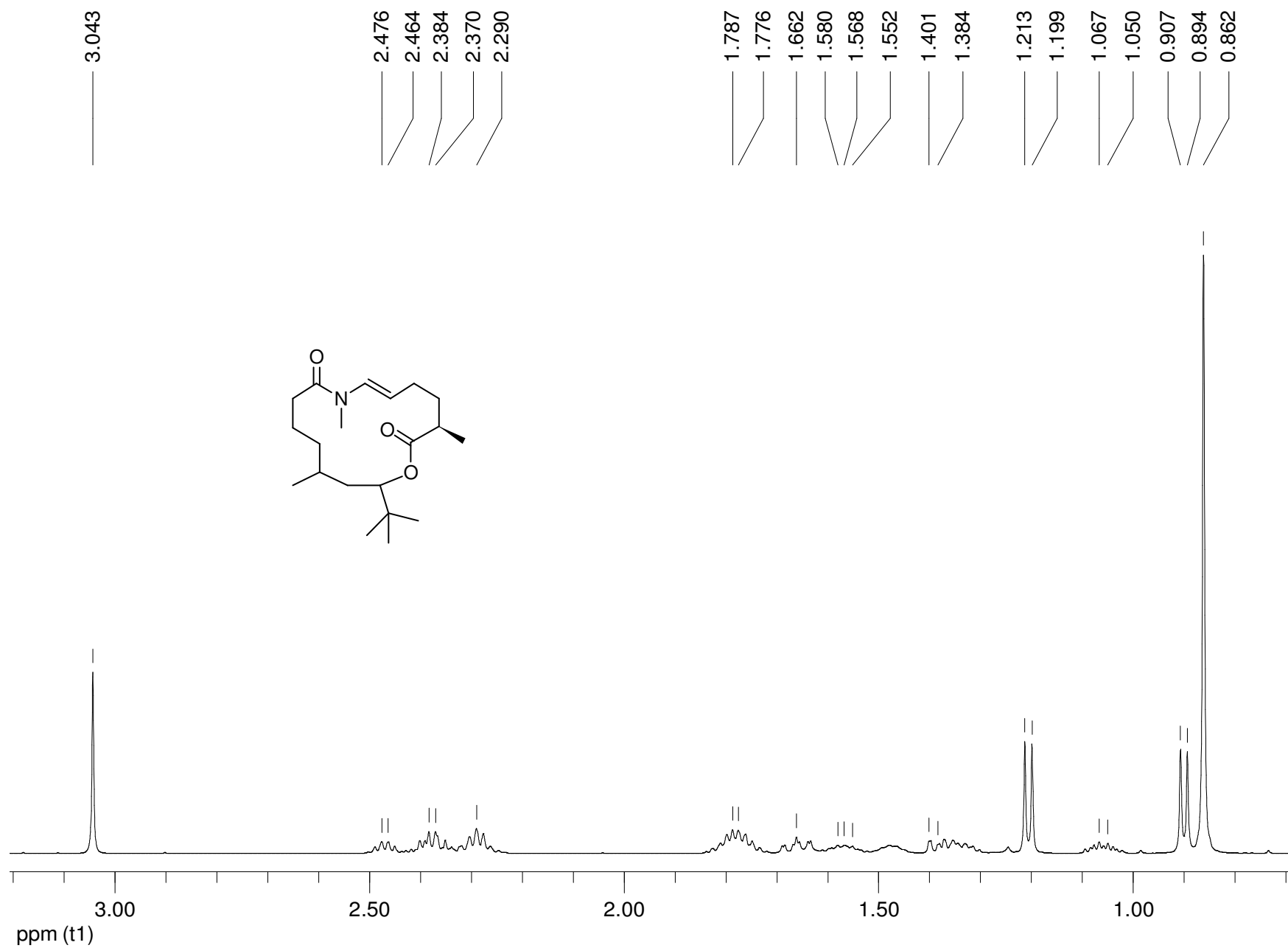


Figure S6.  $^{13}\text{C}$  NMR spectrum of Palmyrolide A (**1**) (in  $\text{CDCl}_3$  at 125 MHz).

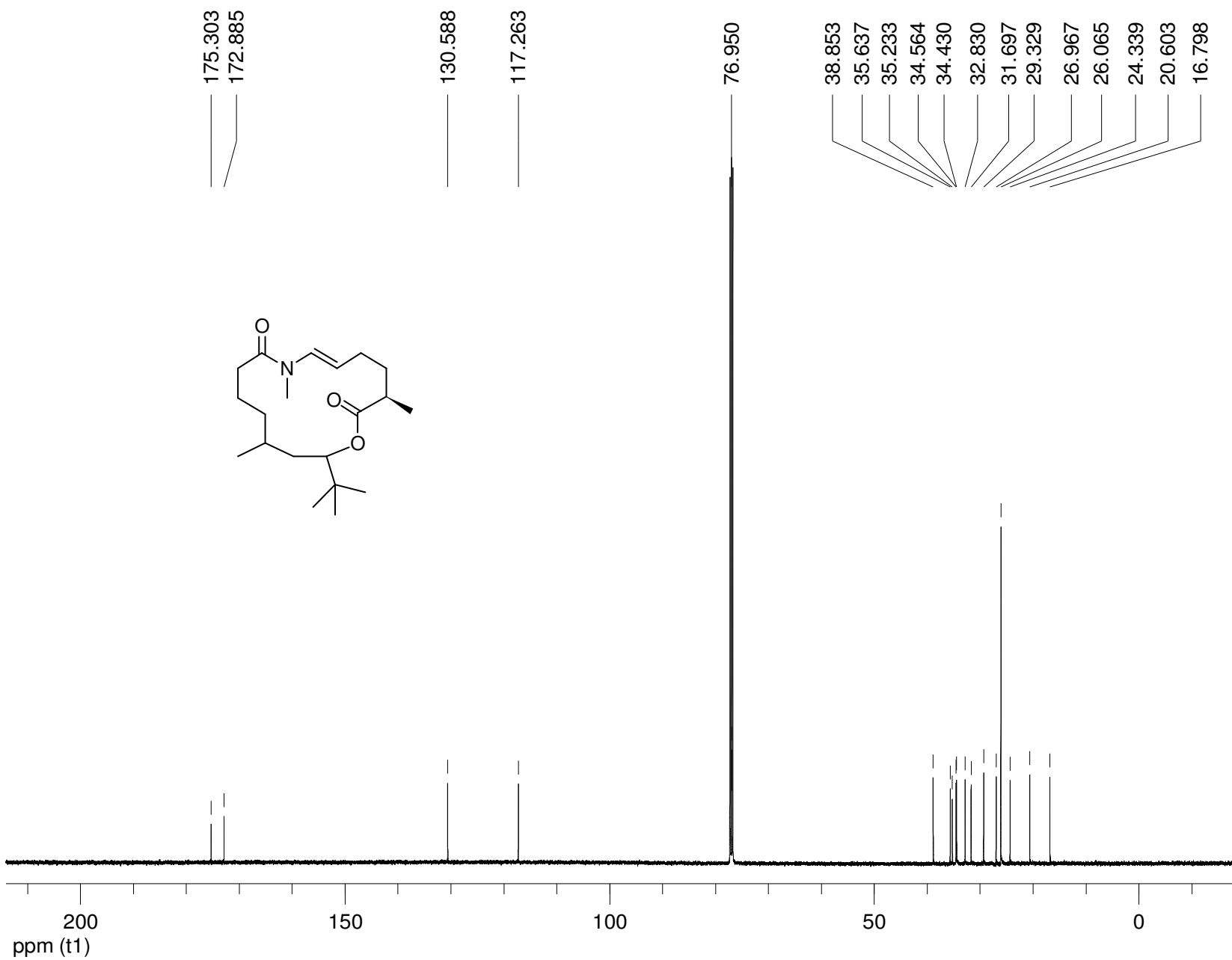


Figure S7. DQF-COSY spectrum of Palmyrolide A (**1**) (in CDCl<sub>3</sub> at 600 MHz).

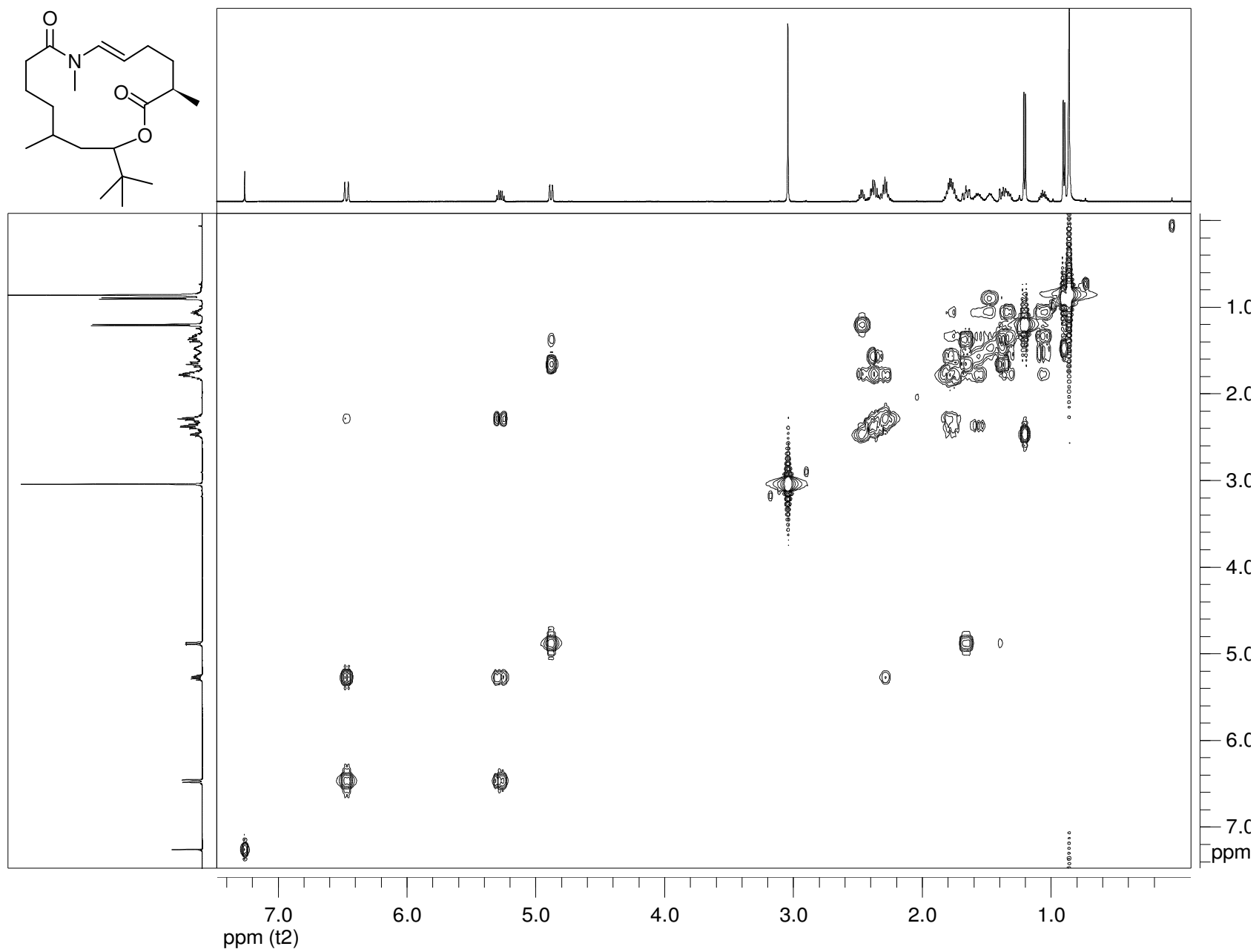


Figure S8. HSQC spectrum of Palmyrolide A (**1**) (in CDCl<sub>3</sub> at 600 MHz).

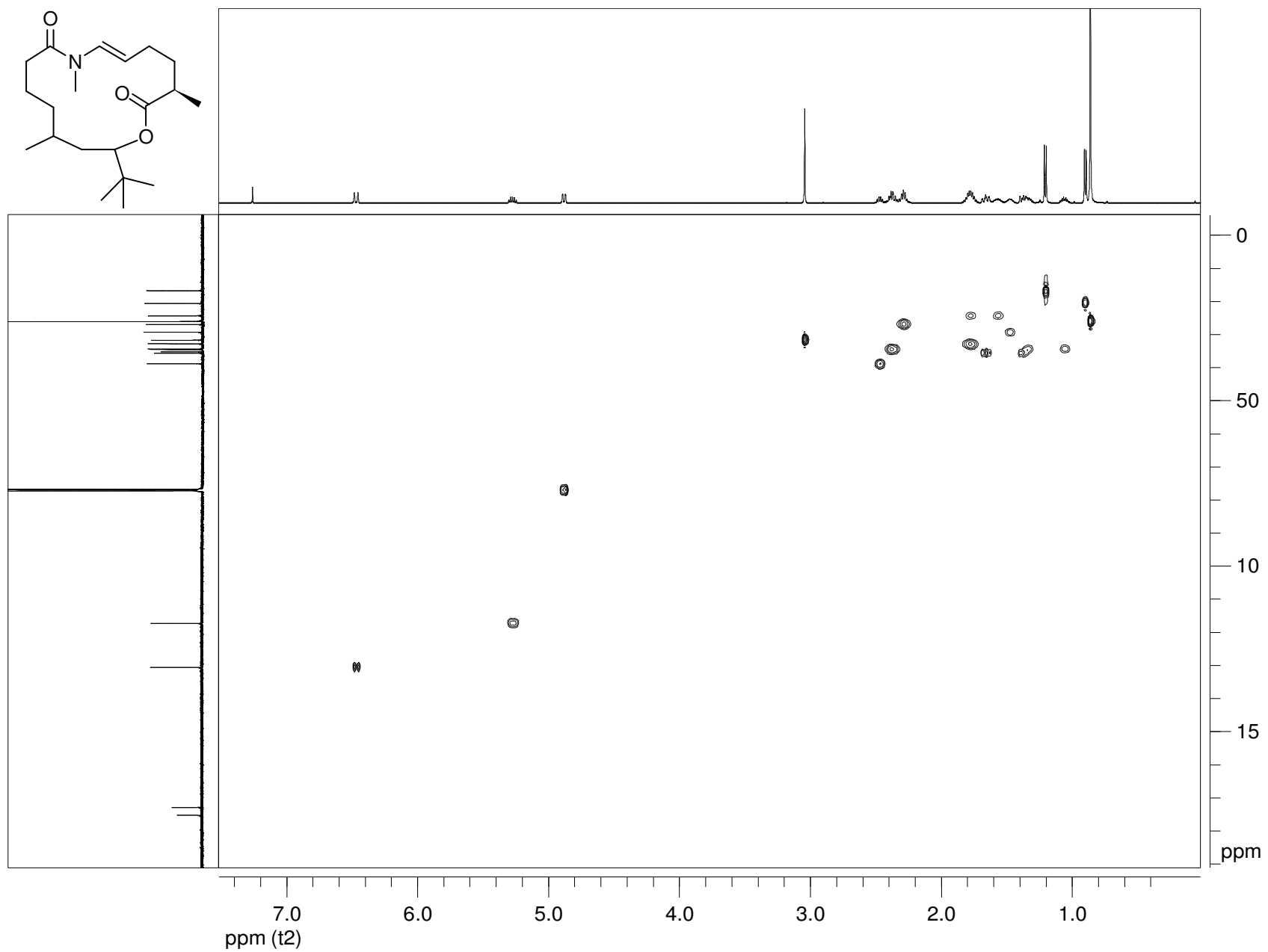




Figure S9. HMBC spectrum of Palmyrolide A (1) (in CDCl<sub>3</sub> at 600 MHz).

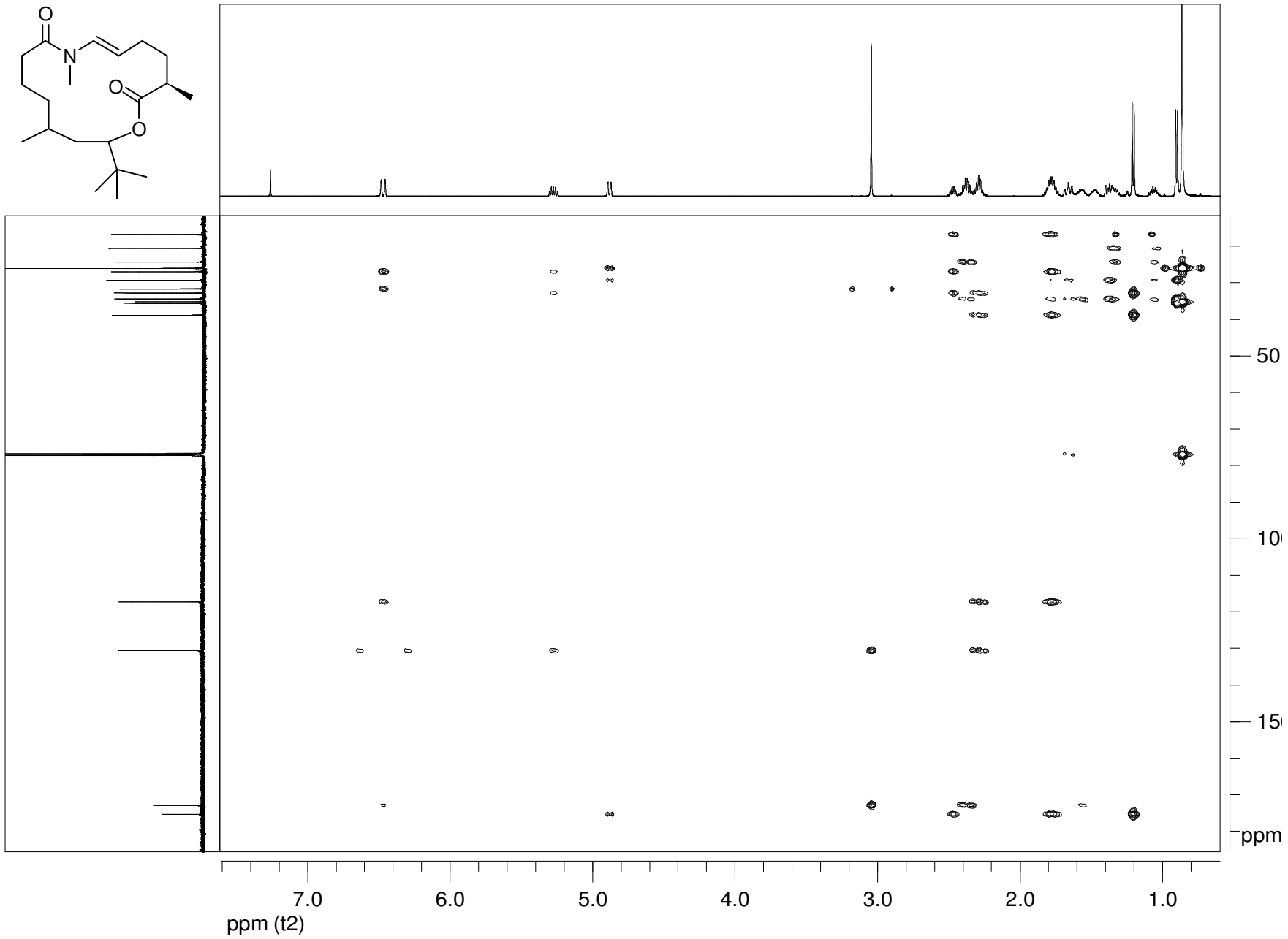


Figure S10. NOESY spectrum of Palmyrolide A (**1**) (in  $\text{CDCl}_3$  at 600 MHz).

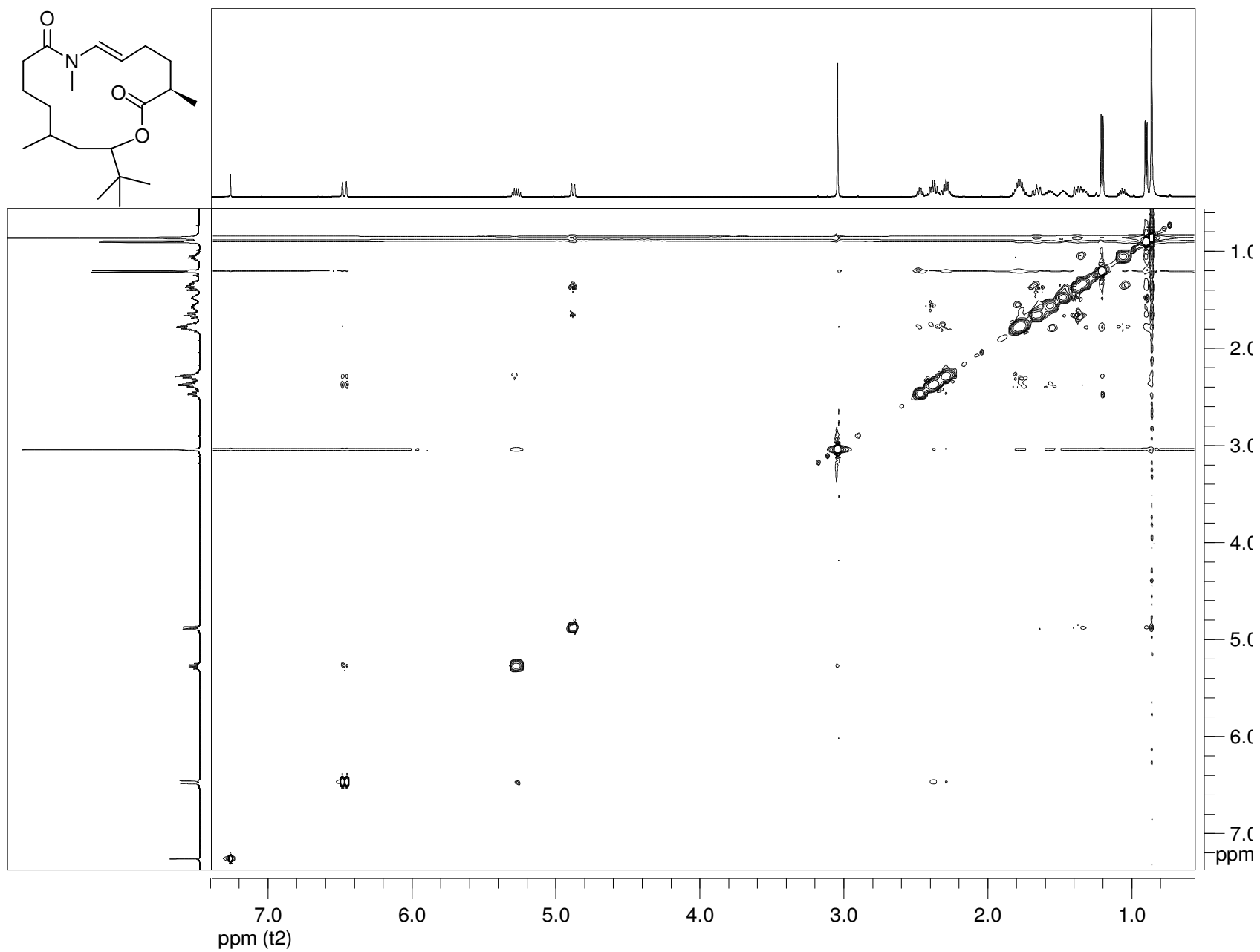


Figure S11.  $^1\text{H}$  NMR spectrum of **2** (in  $\text{CDCl}_3$  at 600 MHz)

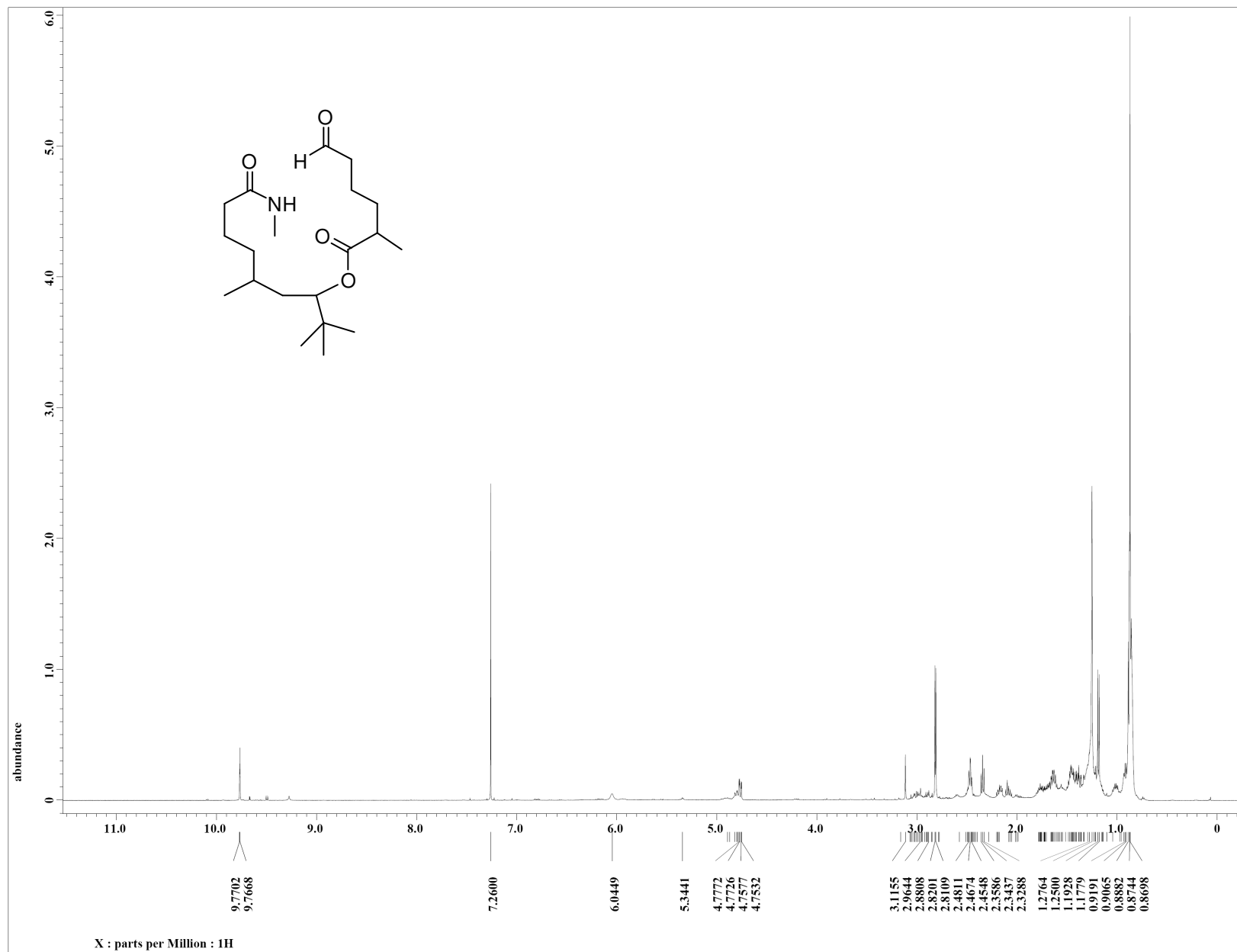


Figure S12. DQF-COSY spectrum of **2** (in  $\text{CDCl}_3$  at 600 MHz)

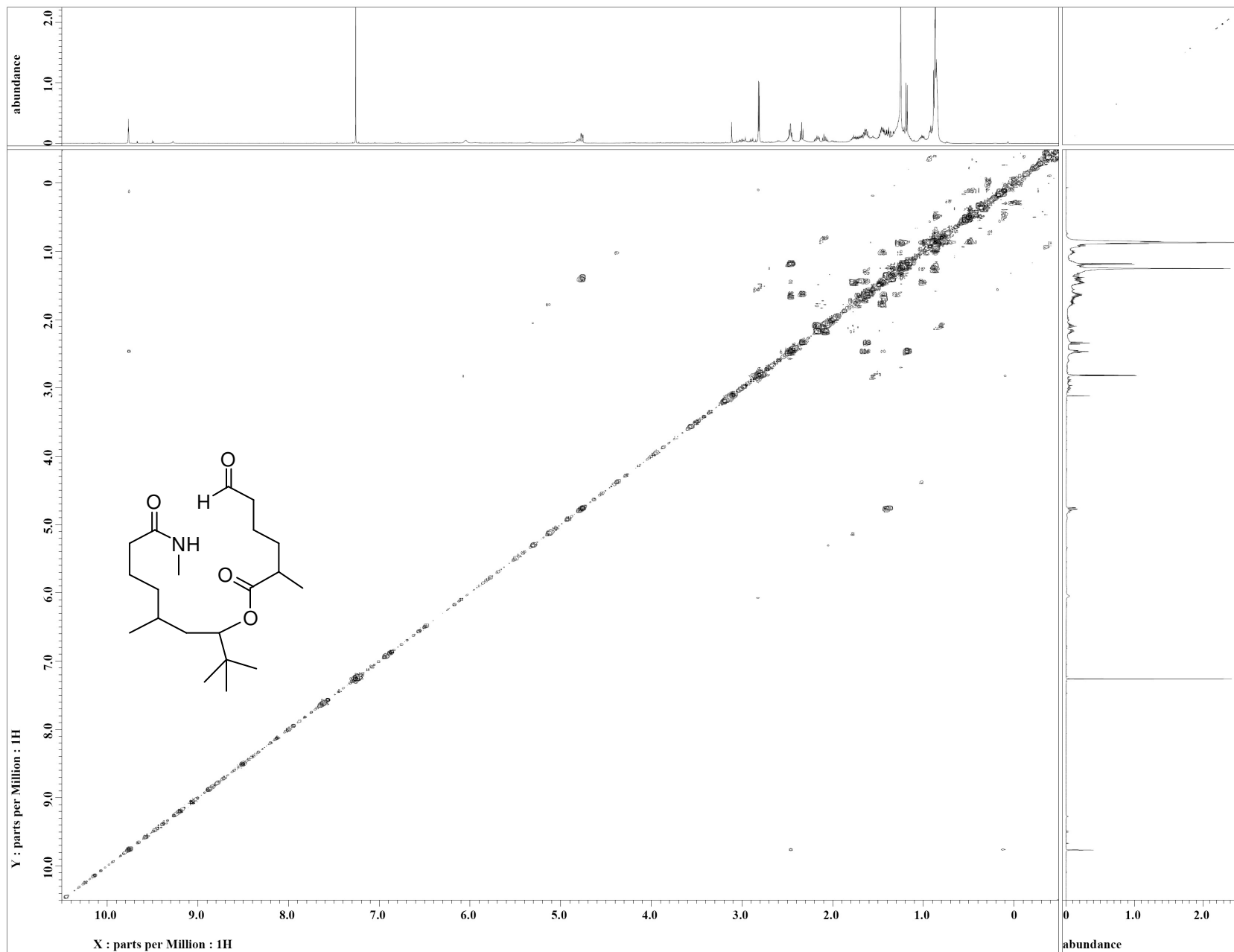


Figure S13. HSQC spectrum of **2** (in CDCl<sub>3</sub> at 600 MHz)

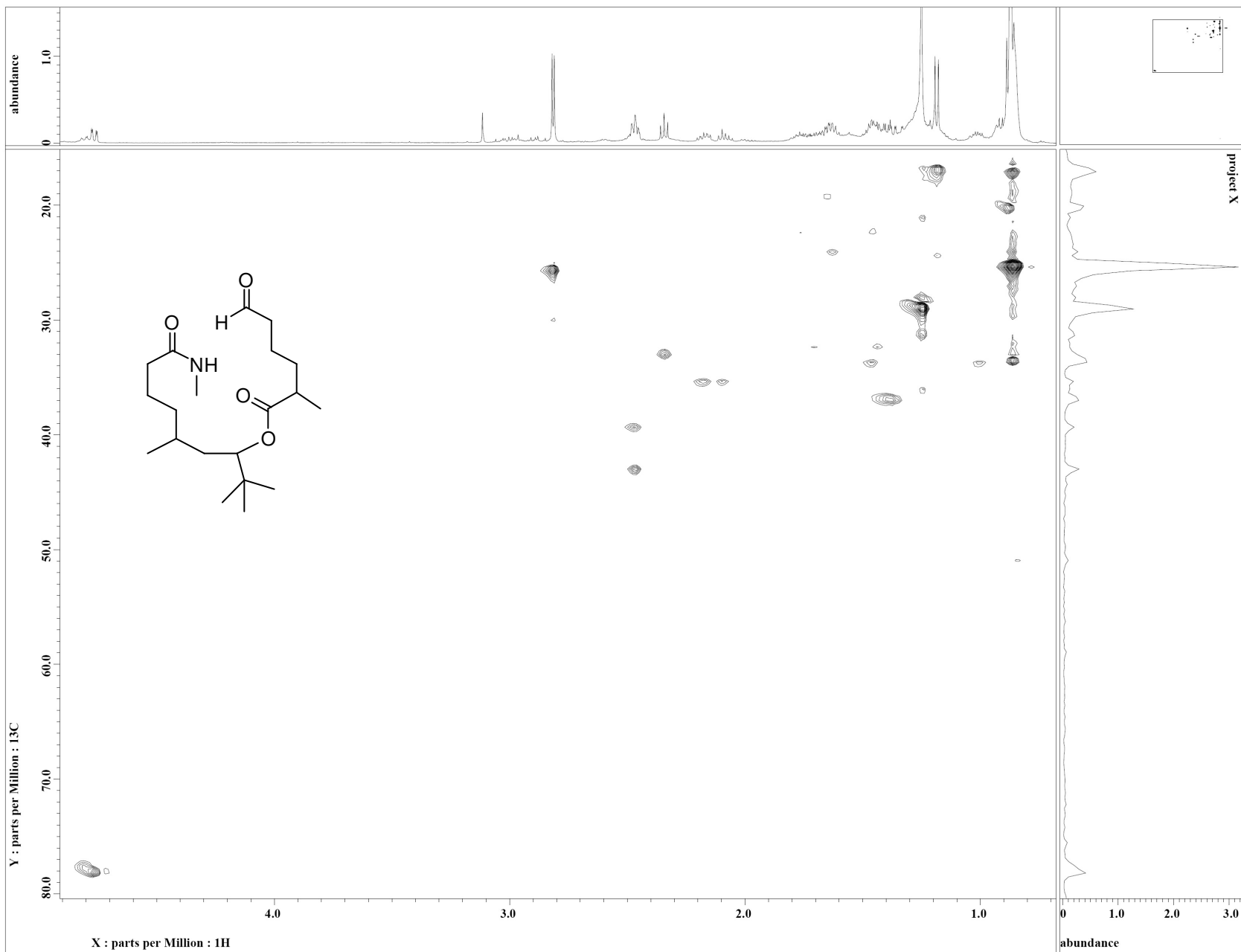


Figure S14. HMBC spectrum of **2** (in CDCl<sub>3</sub> at 600 MHz)

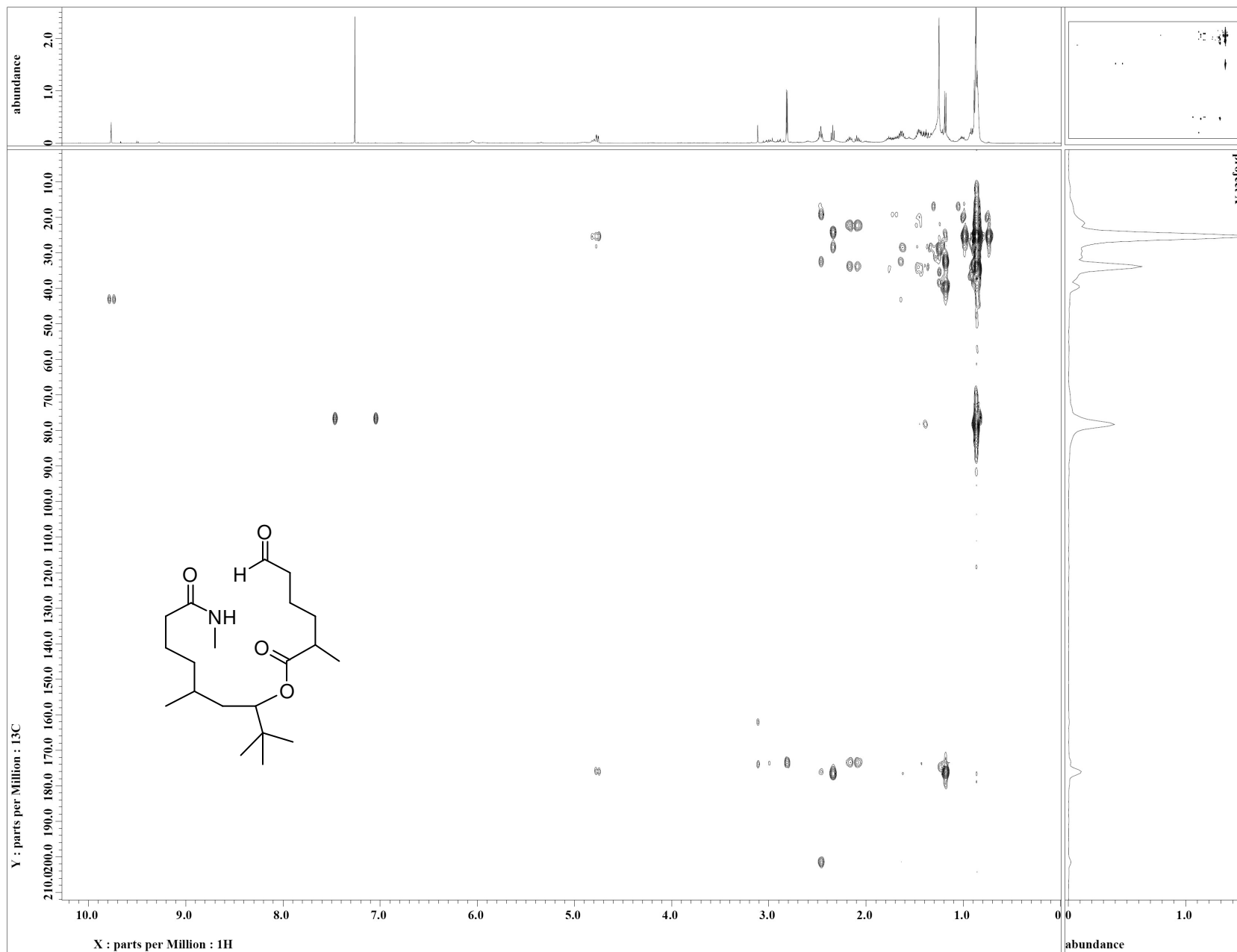


Figure S15.  $^1\text{H}$  NMR spectrum of the Palmyrolide A derivative **4** (in  $\text{CDCl}_3$  at 500 MHz).

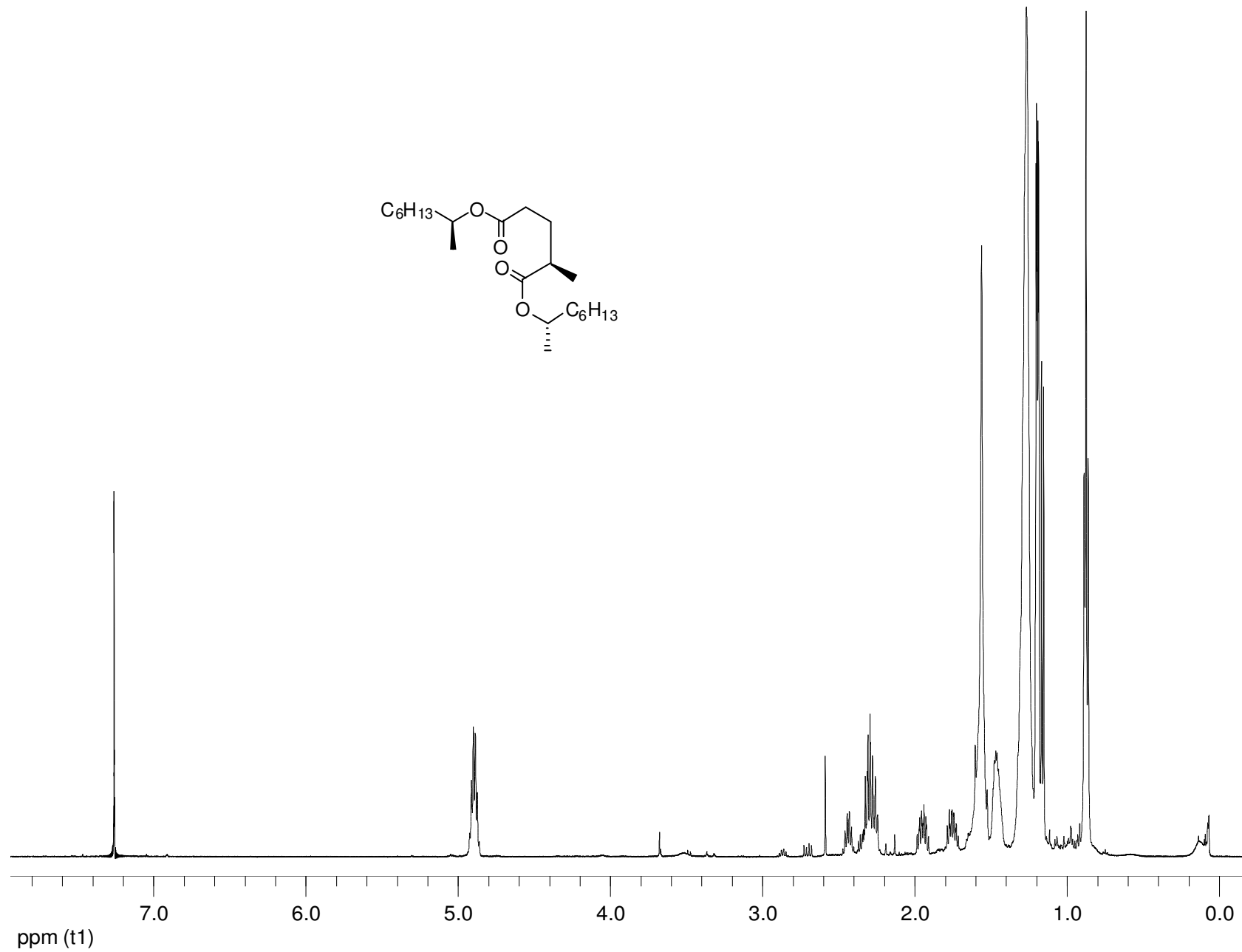


Figure S16.  $^{13}\text{C}$  NMR spectrum of the Palmyrolide A derivative **4** (in  $\text{CDCl}_3$  at 125 MHz).

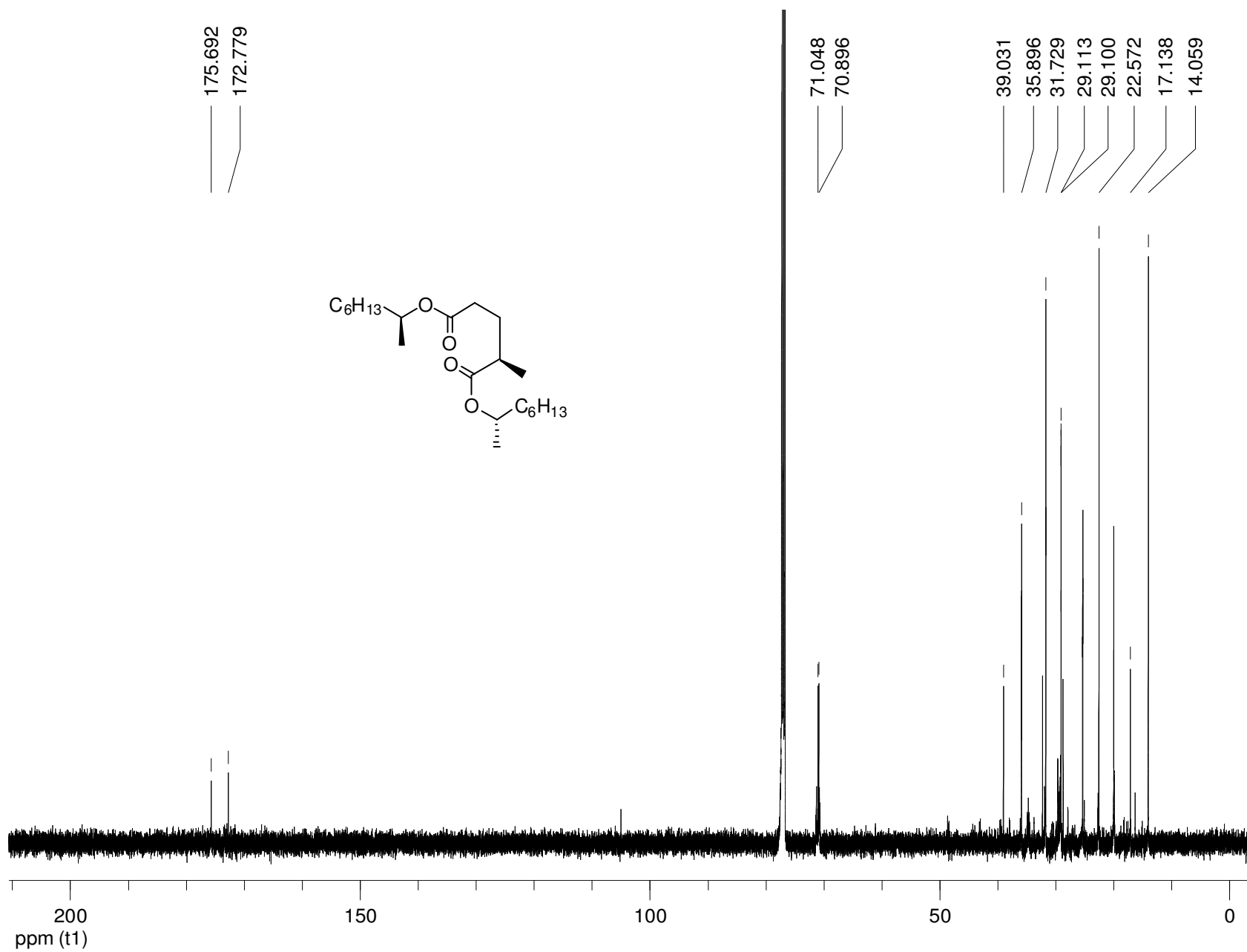




Figure S17.  $^1\text{H}$  NMR spectrum of standard (2*R*,1'*S*,1''*S*)-4 (in  $\text{CDCl}_3$  at 500 MHz).

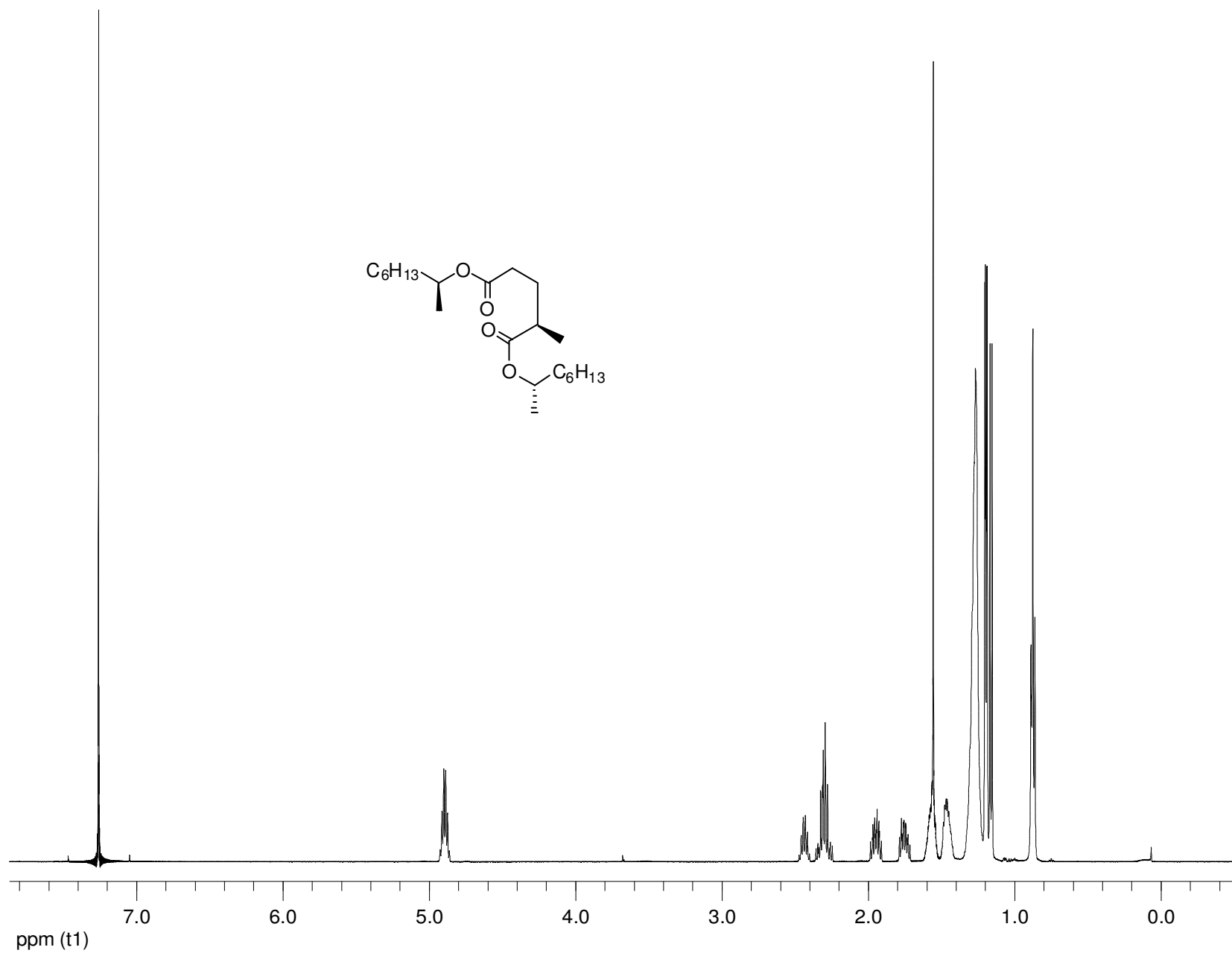


Figure S18.  $^{13}\text{C}$  NMR spectrum of standard (2*R*,1'*S*,1''*S*)-**4** (in  $\text{CDCl}_3$  at 125 MHz).

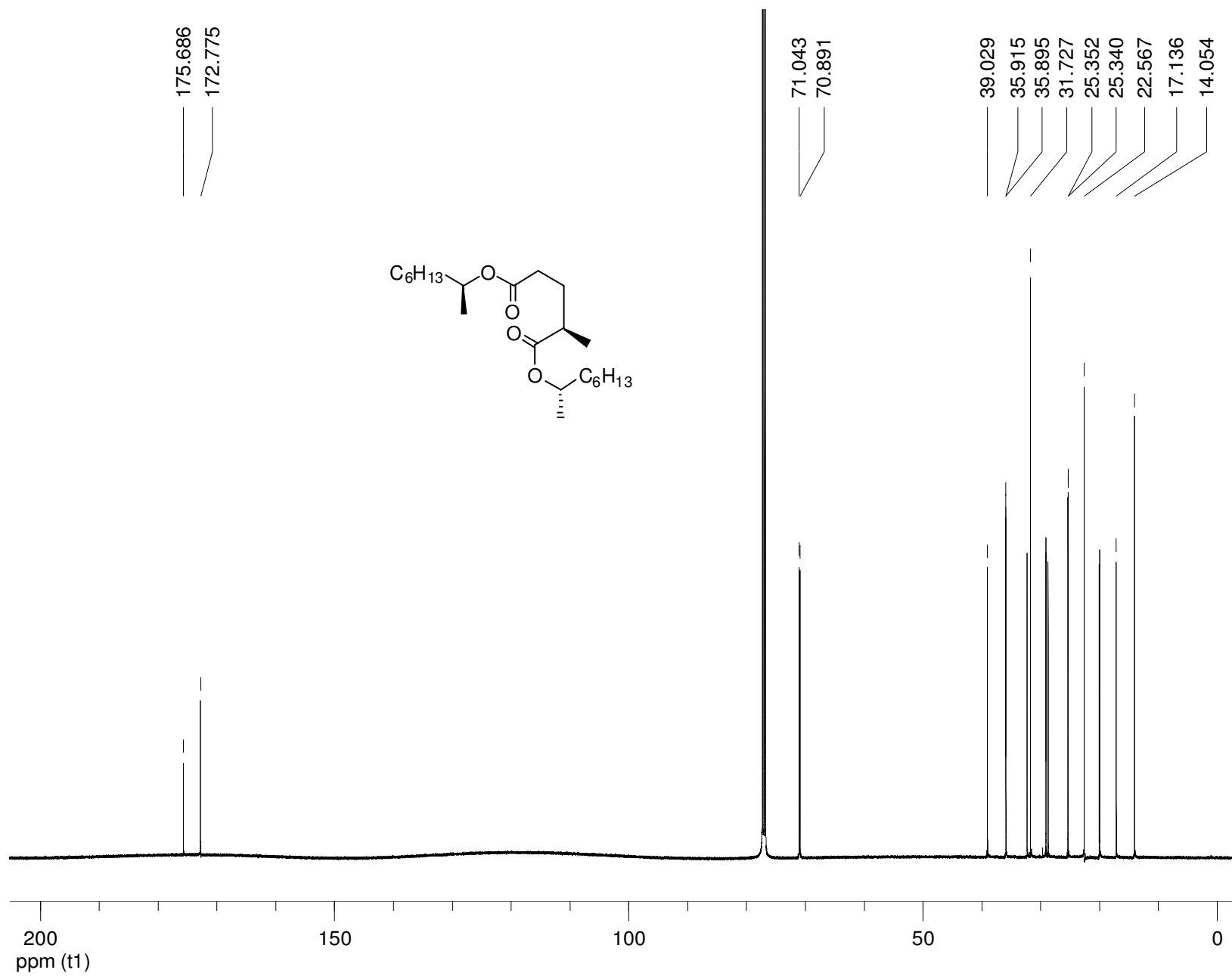


Figure S19.  $^1\text{H}$  NMR spectrum of standard (2*S*,1'*S*,1''*S*)-**4** (in  $\text{CDCl}_3$  at 500 MHz).

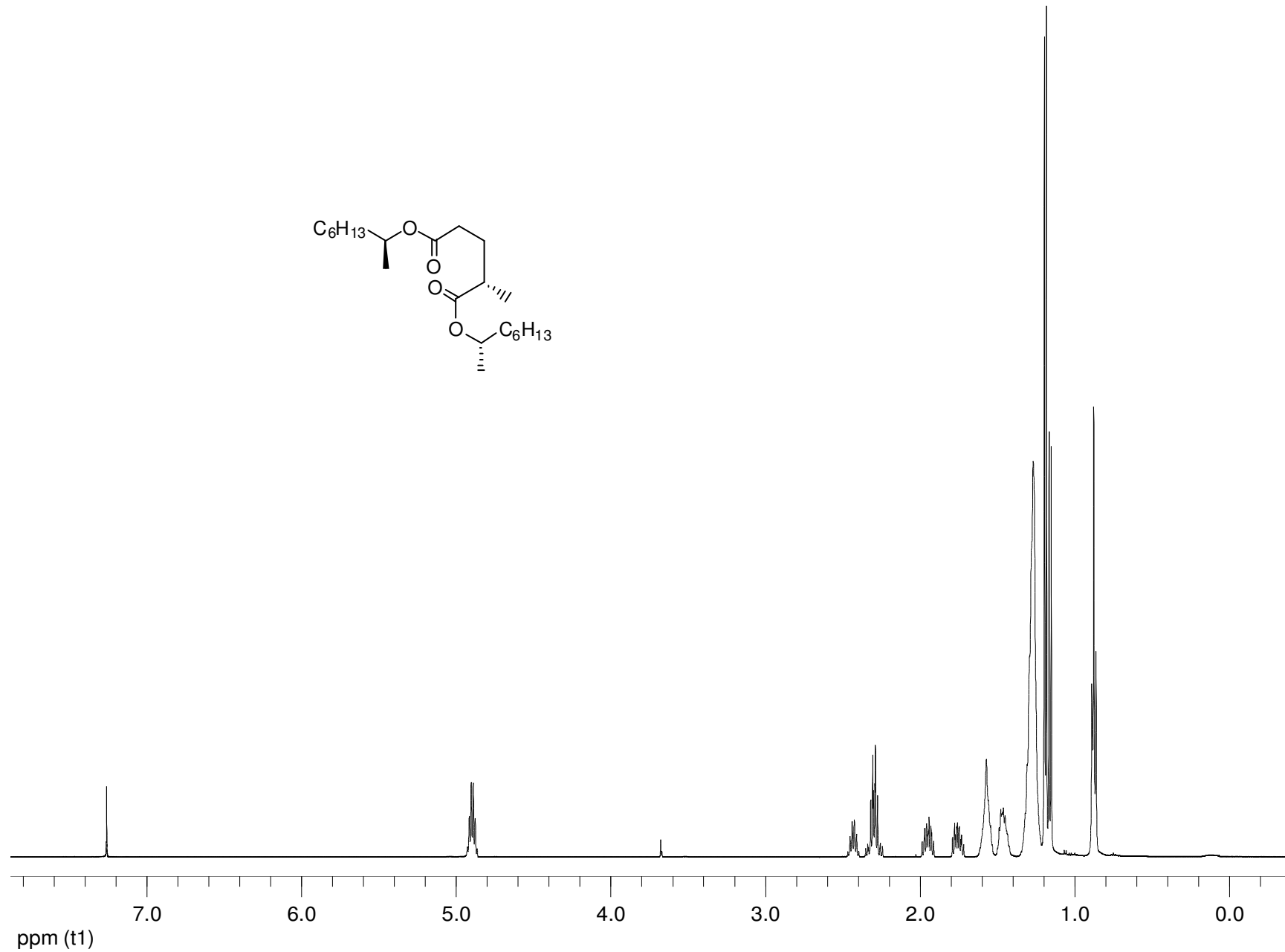


Figure S20.  $^{13}\text{C}$  NMR spectrum of standard (2*S*,1'*S*,1''*S*)-4 (in  $\text{CDCl}_3$  at 125 MHz).

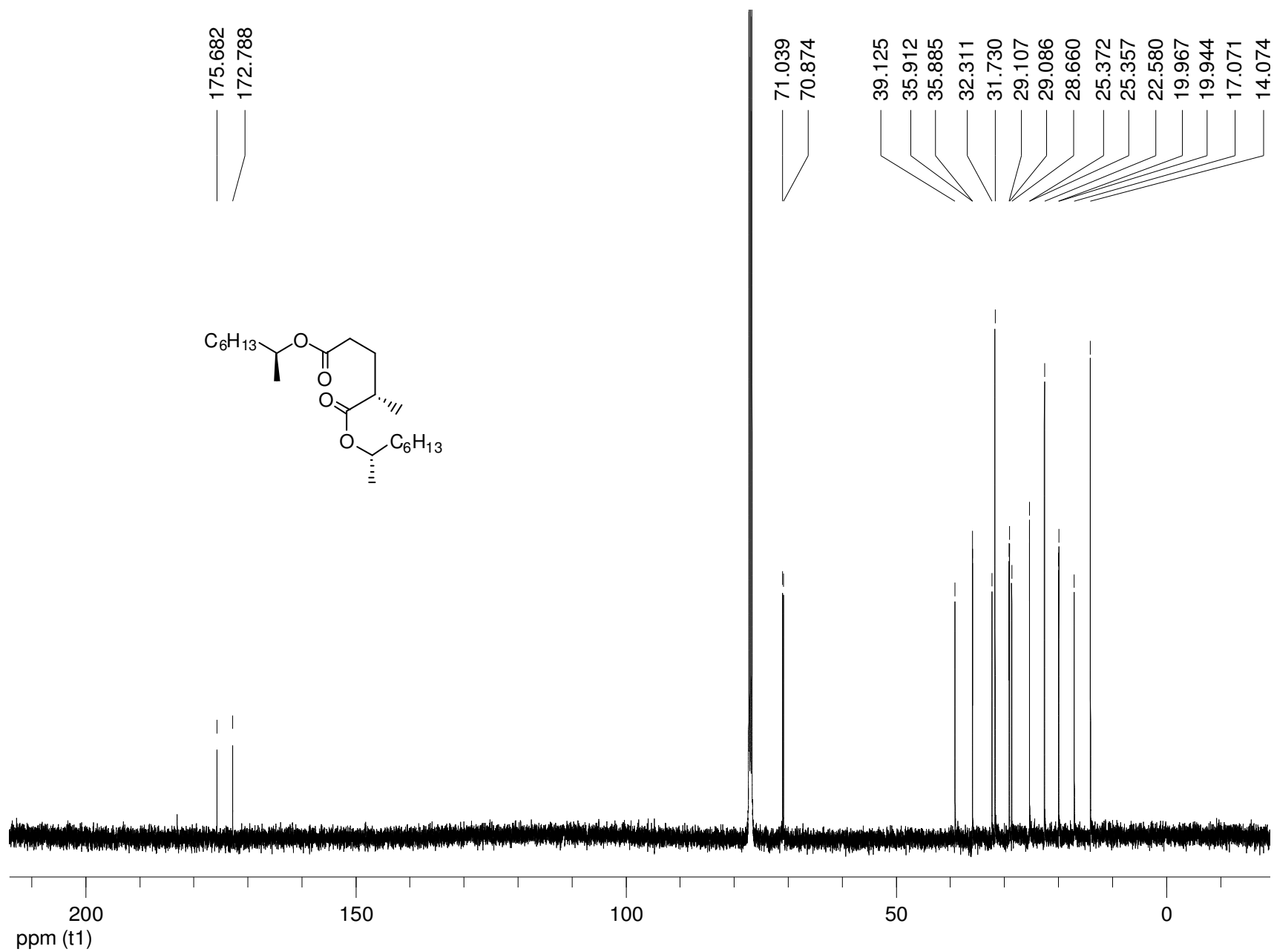


Figure S21. Comparison of  $^1\text{H}$  NMR spectra for derivative **4**, standard (2*R*,1'*S*,1''*S*)-**4**, and standard (2*S*,1'*S*,1''*S*)-**4** (in  $\text{CDCl}_3$  at 500 MHz).

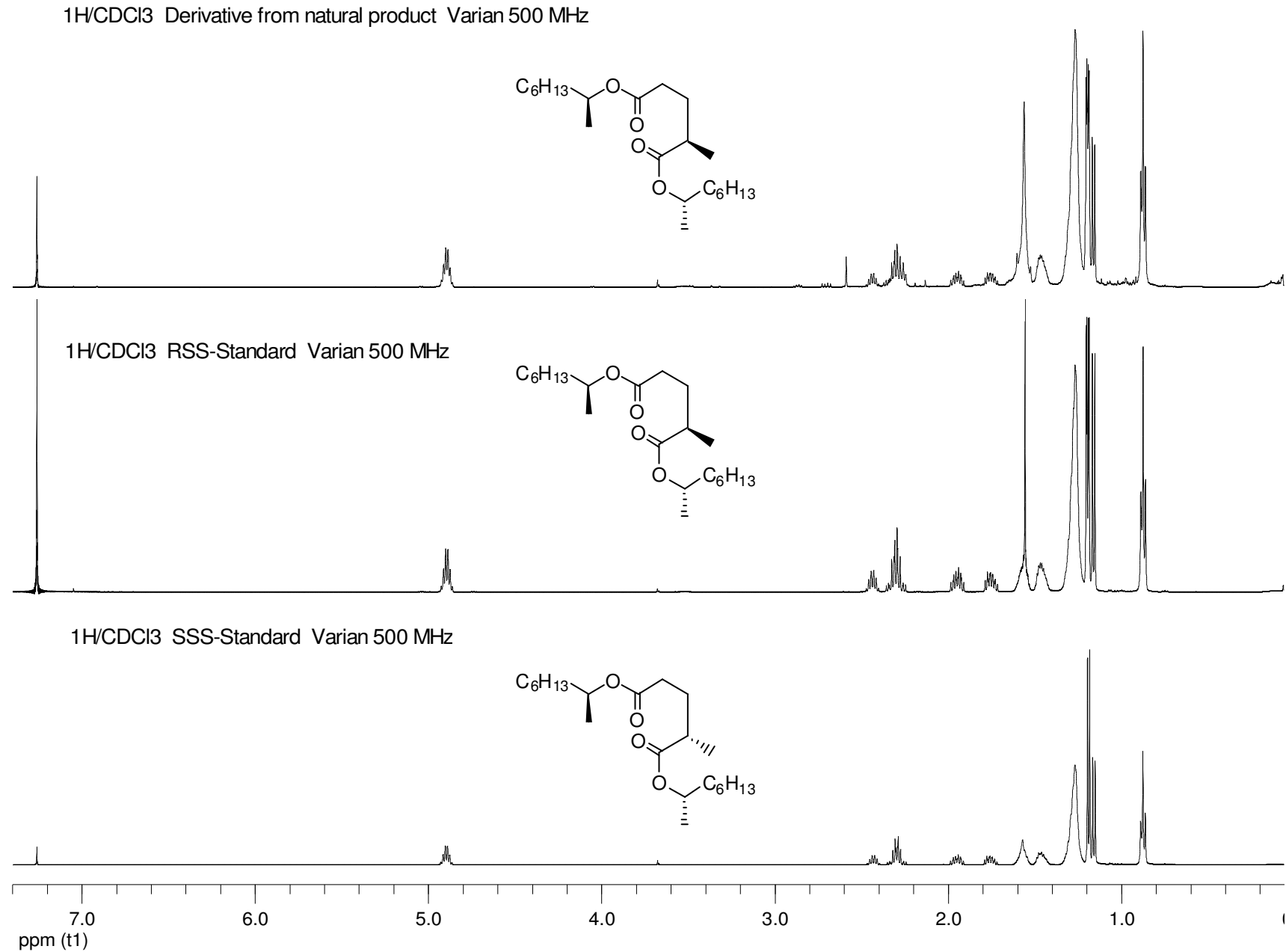
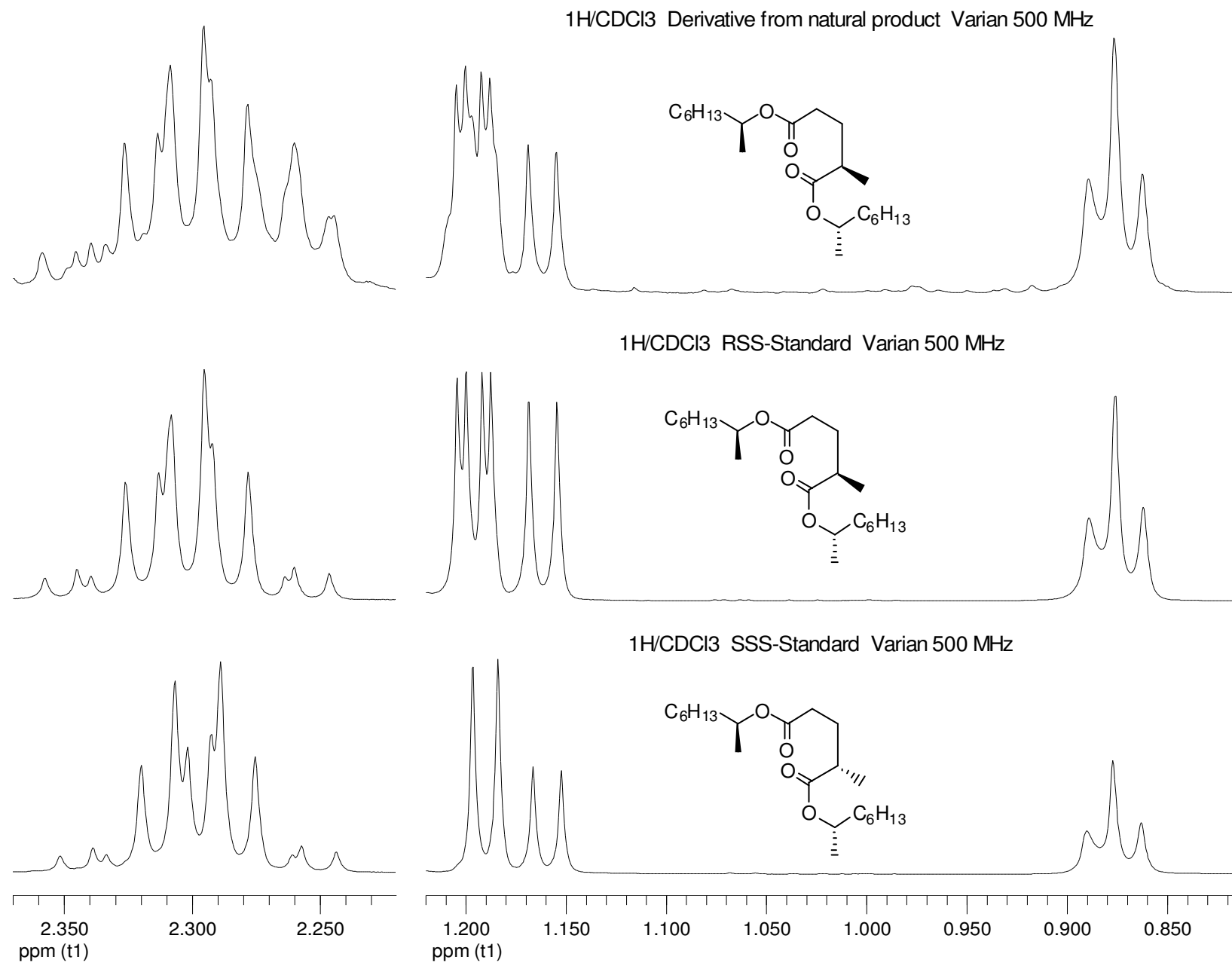


Figure S22. Comparison of key  $^1\text{H}$  NMR resonances for derivative **4**, standard (2*R*,1'*S*,1''*S*)-**4**, and standard (2*S*,1'*S*,1''*S*)-**4** (in  $\text{CDCl}_3$  at 500 MHz).



## Bioassay data

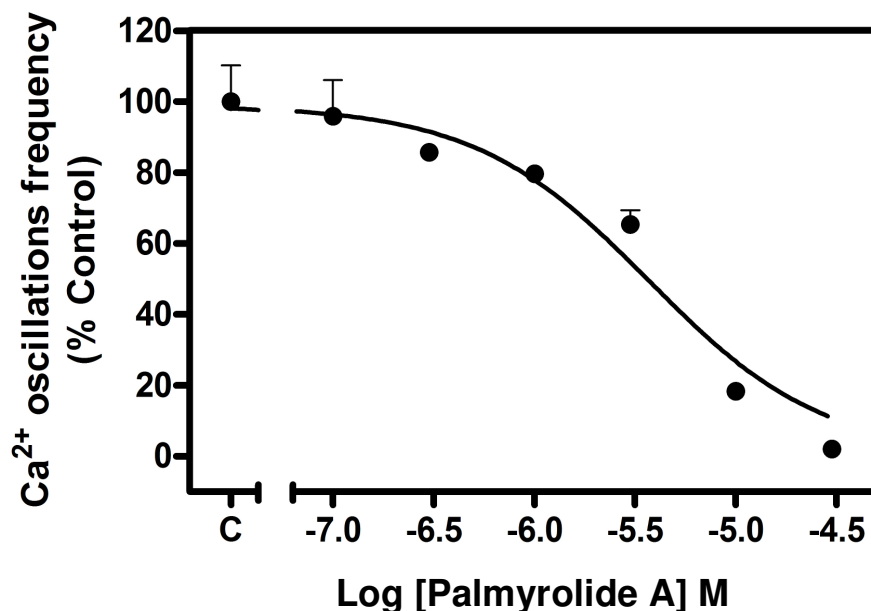


Figure S23. Concentration-response profile for palmyrolide A (**1**)-induced suppression in the frequency of spontaneous  $\text{Ca}^{2+}$  oscillations in mouse cerebrocortical neurons. Depicted is a three-parameter logistic fit to the frequency data that yielded an  $\text{IC}_{50}$  value of  $3.70 \mu\text{M}$  (95% confidence intervals  $2.29\text{-}5.78 \mu\text{M}$ ).

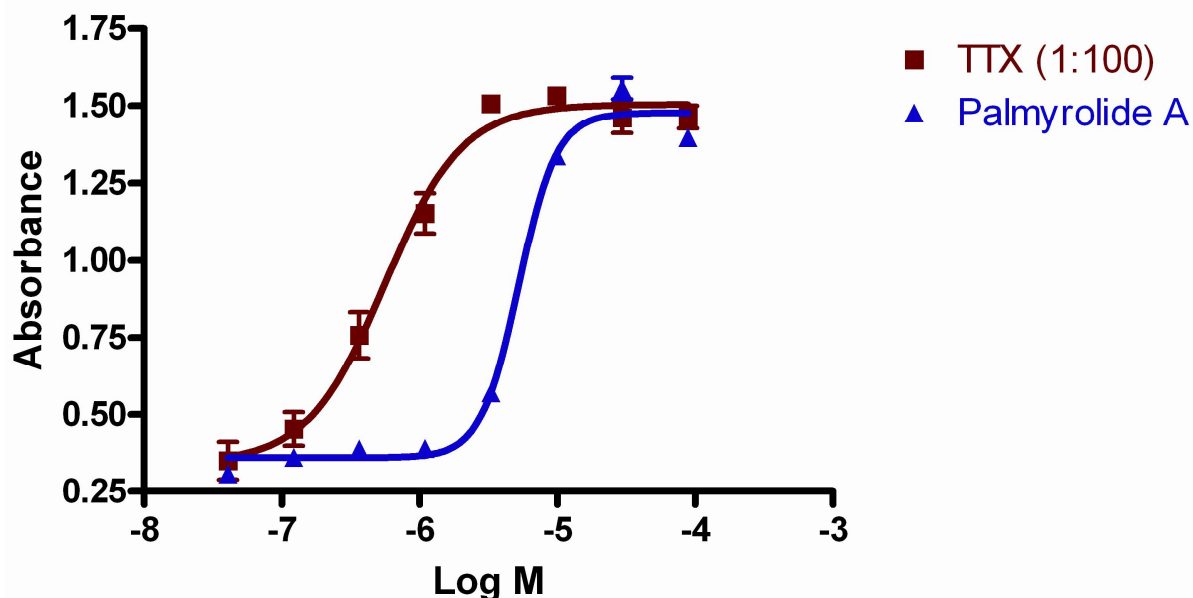


Figure S24. Concentration-response profile for palmyrolide A (**1**)- and tetrodotoxin-induced suppression of sodium overload in mouse neuroblastoma (neuro2a) cells. Veratridine and ouabain were used to increase the concentration of sodium in the cells. The  $\text{IC}_{50}$  values for palmyrolide A (**1**)- and tetrodotoxin were  $5.2$  and  $5.6 \mu\text{M}$ , respectively. TTX was diluted 100 times to reach a similar activity profile as **1**.

## References

- (1) (a) Klein, D.; Braeckman, J. C.; Daloz, D. *Tetrahedron Lett.* **1996**, *37*, 7519-7520. (b) Klein, D.; Braeckman, J. C.; Daloz, D.; Hoffmann, L.; Castillo, G.; Demoulin, V. *J. Nat. Prod.* **1999**, *62*, 934-936.
- (2) Castenholz, R. W. *Bergey's Manual of Systematic Bacteriology*, 2nd ed. Springer: New York, 2001, p 487-493.
- (3) Komárek, J.; Anagnostidis, K. In *Süßwasserflora von Mitteleuropa*; Büdel, B.; Gärtner, G.; Krienitz, L.; Schagerl, M., eds. 2005, vol 19/2, p 441-625.
- (4) Edgar, R.C. *BMC Bioinformatics.* **2004**, *32*, 1792-1797.
- (5) Cannone, J. J.; Subramanin, S.; Schnare, M. N.; Collett, J. R.; D'Souza, L. M.; Du, Y.; Feng, B.; Lin, N.; Madabusi, L. V.; Muller, K. M.; Pnde, N.; Schang, Z.; Yu, N.; Gutell R. R. *BMC Bioinformatics* **2002**, *3*, 1471-2105.
- (6) Posada, D.; Crandall, K. A. *Bioinformatics* **1998**, *14*, 817-818.
- (7) Guindon, S.; Gascuel O. *System. Biol.* **2003**, *52*, 696-704, 2003.
- (8) Ronquist, F.; Huelsenbeck, J. P. *Bioinformatics* **2003**, *12*, 1572-1574.